A secondary metabolite drives intraspecies antagonism in a gut symbiont that is inhibited by peptidoglycan acetylation

Mustafa Özçam[1,2], Jee-Hwan Oh[1], Restituto Tocmo[1,3], Deepa Acharya[4], Shenwei Zhang[1], Silvette Ruiz-Ramírez[1], Fuyong Li[5], Christopher C. Cheng[6], Eugenio Vivas[7], Federico E. Rey[7], Jan Claesen[8], Tim Bugni[4], Jens Walter[5,6,9,10], Jan-Peter van Pijkeren[1,11*]

[1] Department of Food Science, University of Wisconsin-Madison, Madison, WI, 53706, USA

[2] Division of Gastroenterology, Department of Medicine, University of California San Francisco, CA, 94141, USA.

[3] Present Address: Department of Pharmacy Practice, University of Illinois at Chicago, Chicago, IL, 60612, USA

[4] Department of Pharmacy, University of Wisconsin-Madison, Madison, WI, 53706, USA

[5] Department of Agriculture, Food and Nutritional Science, University of Alberta, Edmonton, AB T6G 2P5, Canada

[6] Department of Biological Sciences, University of Alberta, Edmonton, AB T6G 2P5, Canada;

[7] Department of Bacteriology, University of Wisconsin-Madison, Madison, WI, 53706, USA

[8] Department of Cardiovascular and Metabolic Sciences and Center for Microbiome and Human Health, Lerner Research Institute, Cleveland Clinic, Cleveland, OH, 44195, USA

[9] Department of Medicine and APC Microbiome Ireland, University College Cork, Cork T12 K8AF, Ireland;

[10] School of Microbiology, University College Cork, Cork T12 YT20, Ireland.

[11] Lead Contact

*Correspondence: vanpijkeren@wisc.edu

SUMMARY

The mammalian microbiome encodes numerous secondary metabolite biosynthetic gene clusters, yet their role in microbe-microbe interactions is unclear. Here, we characterized two polyketide synthase gene clusters (*fun* and *pks*) in the gut symbiont *Limosilactobacillus reuteri.* The *pks*, but not the *fun* cluster, encodes antimicrobial activity. Forty-one out of 51 *L. reuteri* strains tested are sensitive to Pks products, which was independent of strains' host origin. The sensitivity to Pks was also established in intraspecies competition experiments in gnotobiotic mice. Comparative genome analyses between Pks-resistant and sensitive strains identified an acyltransferase gene (*act*) that is unique to Pks-resistant strains. Subsequent peptidoglycan analysis of the wild-type and the *act* mutant strains showed that Act acetylates peptidoglycan. The *pks* mutants lost their competitive advantage and *act* mutants lost their Pks resistance *in vivo*. Thus, our findings provide mechanistic insights into how closely related gut symbionts can compete and co-exist in the gastrointestinal tract.

Keywords: *Limosilactobacillus reuteri,* gut symbiont, polyketide, polyene, secondary metabolite,biosynthetic gene clusters, acyltransferase, antimicrobial, acetylation, microbial competition

INTRODUCTION

The mammalian gastrointestinal tract is inhabited by trillions of microorganisms that coexist with their host (Sender et al., 2016). While factors like host genetics, immune status, nutritional resources and colonization history affect microbial composition (Bonder et al., 2016; David et al., 2014; Hooper et al., 2015; Martínez et al., 2018; Snijders et al., 2016; Turnbaugh et al., 2009; Zarrinpar et al., 2014), the relationship between microbes is determined by competitive interactions (Boon et al., 2014). Bacteria have developed numerous strategies that mediate survival and competition, including the production of broad and narrow spectrum antimicrobials (Sassone-Corsi et al., 2016). On the other hand, acquisition of resistance genes and/or modification of the cell wall can help bacteria survive the antimicrobial warfare in the gut (Murray and Shaw, 1997).

Some bacterial secondary metabolites have antimicrobial activity against other community members. Their interactions—known as interference competition—are important in the assembly and the maintenance of microbial communities (Jacobson et al., 2018). Most secondary metabolites are produced by biosynthetic gene clusters (BGCs) and polyketide synthase (PKS) gene clusters form a prominent subclass, involved in the biosynthesis of carbon chain backbones from the repeated condensation of acyl-CoA building blocks (Lin et al., 2015; Medema et al., 2014). A survey of 2,430 reference genomes from the Human Microbiome Project uncovered more than 3,000 BGCs (Donia et al., 2014). So far, only seven PKS-like BGCs encoded by gut-associated bacteria have been functionally characterized (Figure S1).

As a class of polyketide synthase products, aryl polyenes are lipids with an aryl head group conjugated to a polyene tail (Lin et al., 2015) and are widely distributed in soil and host-associated bacteria (Cimermancic et al., 2014; Youngblut et al., 2020). Although, many polyene

compounds isolated from terrestrial and marine microbes possess antimicrobial affects *in vitro* (Herbrík et al., 2020; Lee et al., 2020; Li et al., 2021; Zhao et al., 2021), virtually nothing is known about their ecological role in microbe-host and microbe-microbe interactions in the mammalian gastrointestinal tract (Aleti et al., 2019). While metagenome studies are critically important to identify novel polyene-like BGCs within the microbiome (Hiergeist et al., 2015; Medema et al., 2011), the assessment of model organisms and their isogenic mutants in the appropriate ecological context is critical to advance our knowledge on the biological function of these BGC-derived compounds.

Limosilactobacillus reuteri, until recently known as *Lactobacillus reuteri* (Zheng et al., 2020) is a gut symbiont species that inhabits the gastrointestinal tract of various vertebrates, including rodents, birds and primates (Duar et al., 2017). This, combined with the available genome editing tools (Oh and Van Pijkeren, 2014; Van Pijkeren et al., 2012; Zhang et al., 2018), make *L. reuteri* an ideal model organism to study microbe-microbe, microbe-phage and microbe-host interactions (Lin et al., 2018; Oh et al., 2019; Özçam et al., 2019; Walter et al., 2011). Previously, we identified two genetically distinct PKS clusters (*pks* and *fun*) in *L. reuteri* R2lc that activated the Aryl Hydrocarbon Receptor (Özçam and van Pijkeren, 2019).

In this study, we found that the *pks* cluster in *L. reuteri* R2lc encodes antimicrobial activity. Intraspecies competition experiments in gnotobiotic mice with the wild-type and the *pks* deletion mutant revealed that Pks expression can provide a competitive advantage. Remarkably, a small number *L. reuteri* strains were resistant to the antimicrobial activity of Pks. We discovered this resistance was driven by a gene encoding an acetyltransferase gene that increases peptidoglycan acetylation. Thus, our findings uncovered mechanisms by which gut symbionts

can compete and co-exist with closely related strains through secondary metabolite production and cell-wall modification.

RESULTS

L. reuteri Pks inhibits the competitor strain

The rodent isolate *L. reuteri* R2lc contains two PKS clusters, *fun* and *pks* (Figure 1A). In both the human and rodent gut ecosystem, *L. reuteri* R2lc outcompetes most *L. reuteri* strains, including the rodent isolate *L. reuteri* 100-23 (Duar et al., 2017; Oh et al., 2009). Because select PKS products have antimicrobial activity (Lin et al., 2015), we tested to what extent Pks and Fun provide strain R2lc with a competitive advantage. We performed *in vitro* competition experiments in batch cultures using 1:1 mixtures of the rodent gut isolates *L. reuteri* 100-23 and *L. reuteri* R2lc wild type, or our previously generated PKS mutants (R2lcΔ*fun* or R2lcΔ*pks*) (Özçam et al., 2019). Following 24 hours of incubation, the mixed cultures were plated. On agar, R2lc and its derivatives form pigmented colonies, while 100-23 colonies are opaque color in appearance. Co-incubation of R2lc + 100-23 or R2lcΔ*fun* + 100-23 only recovered pigmented colonies; however, co-incubation of R2lcΔ*pks* + 100-23 yielded a mixture of pigmented and opaque colonies (% pigmented:opaque colony distribution is 29:71) (Figure 1B). These data suggest that R2lc *pks* but not *fun* cluster provides strain R2lc with a competitive advantage when co-cultured with *L. reuteri* 100-23.

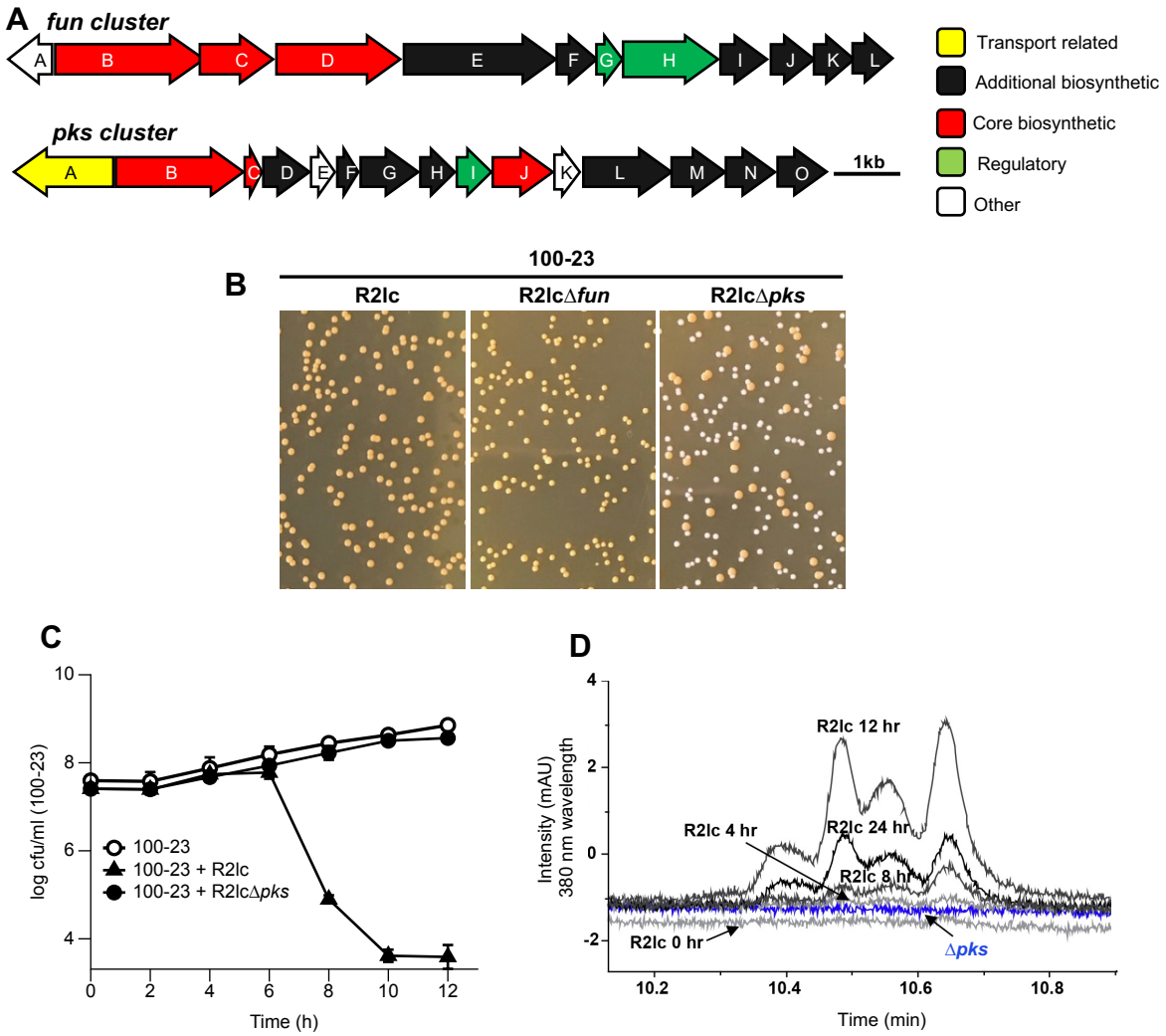

Figure 1. A polyketide synthase cluster in *L. reuteri* R2lc produces polyene-like compounds and provides competitive advantage A) The *fun* cluster (top) spans 13.4 kb containing 12 Open Reading Frames (ORFs), and the *pks* cluster (bottom) spans 11.3 kb containing 15 ORFs. Transport-related, additional biosynthetic, regulatory, and other genes are represented by different colors. **B)** R2lc and R2lcΔ*fun* but not R2lcΔ*pks* inhibits *L. reuteri* 100-23. **C)** R2lc has bactericidal effect against 100-23. Single culture (OD_{600}=0.1) or co-cultures (OD_{600}=0.05 from each strain) were mixed and incubated in MRS broth (pH: 4.0, 37°C) and samples were collected

every two hours for up to 12 hours. The data represents the average of three independent experiments. Error bars represents standard deviation. **D)** UPLC-PDA-MS analysis of R2lc and Δ*pks* mutant. R2lc but not Δ*pks* produces unique compounds with a maximum absorption of 380nm (Black: R2lc, blue: Δ*pks*). See also Figure s3.

L. reuteri Pks has a time-dependent bactericidal effect

To understand the dynamics by which R2lc outcompetes 100-23, we performed a time course competition experiment in batch cultures. Mixtures (1:1, OD_{600} = 0.05 per strain) were prepared of R2lc + 100-23, and R2lcΔ*pks* + 100-23. As a control, a monoculture of 100-23 was grown. We harvested samples every two hours and determined the CFU levels. Up to six hours, mixtures of R2lc + 100-23 and R2lcΔ*pks* + 100-23 yielded similar levels of 100-23 colonies, which were comparable to the levels obtained when 100-23 was cultured independently. However, after eight and ten hours of co-incubation of R2lc + 100-23, 100-23 CFU levels were reduced by three and five orders of magnitude, respectively, while 100-23 continued to grow in the R2lcΔ*pks* + 100-23 mixture (Figure 1C). Importantly, the sharp decline in 100-23 CFU counts suggests Pks elicits a strong bactericidal activity against 100-23. Also, the fact that killing of 100-23 is initiated after 6-hours of co-culture suggests that production of Pks may be growth phase dependent.

In mice, *L. reuteri*—including strain 100-23—form a biofilm on the stratified squamous epithelium of the forestomach (Frese et al., 2013; Lin et al., 2018; Savage et al., 1968). Cell numbers of 100-23, R2lc or R2lcΔ*pks* in gastric biofilms were similar ($4.3\times10^8 \pm 2.6\times10^8$, $2.0\times10^8 \pm 3.0\times10^7$, $1.7\times10^8 \pm 4.1\times10^7$ CFU/ml, respectively) (Figure s2A). In biofilm co-cultures, however, R2lc was 750-fold more abundant than 100-23 (P = 0.002). The ability of

R2lc to outcompete 100-23 in biofilm is mediated by Pks, because co-incubation of R2lcΔ*pks* with 100-23 recovered similar levels of CFUs for both strains ($P = 0.27$) (Figure s2B).

L. reuteri pks cluster produces unique polyene-like compounds

To gain more insight into *L. reuteri* R2lc Pks production *in vitro*, we performed Ultra Performance Liquid Chromatography coupled with Photodiode Array and Mass Spectrometer (UPLC-PDA-MS) analysis. By comparing the chromatograms obtained from R2lc and R2lcΔ*pks* cultures, we found that R2lc produces a family of unique compounds with a maximum wavelength of 380 nm. These compounds eluted towards the end of the gradient run where the solvent composition was close to 100% methanol, indicating a hydrophobic characteristic. The large retention time of the compounds on the C18 column and the maximum absorption wavelength are consistent with previously identified polyene compounds (Gruber and Steglich, 2007). Therefore, the putative products of the *pks* cluster are predicted to be polyene compounds.

The UV chromatogram extracted from the R2lc culture at different time points shows an increase in the production of these compounds up to 12 hours of incubation, after which the intensity reduces as shown in samples at 24 hours (Figure 1D). We subsequently analyzed the Liquid Chromatography-Mass Spectrometry (LC-MS) data of R2lc and Δ*pks* samples collected above to identify the polyene products produced by R2lc. The mass spectrum of the peak between 10.52 min – 10.58 min in the R2lc chromatogram at 12 hours clearly showed an ion with *m/z* $[M+H]^+$ value of 257.1172 and corresponding *m/z* $[M+Na]^+$ value of 279.0092, which were absent in the 12-hour culture of *Δpks* (Figure s3). The high-resolution mass for the compound led to the predicted molecular formula of $C_{16}H_{16}O_3$. The reduction of Pks compounds after 12 hours of incubation suggests instability of Pks molecules in our experimental setup.

Taken together, these data suggest that antibacterial compounds are released in a time-dependent manner.

L. reuteri Pks molecules provide a competitive advantage *in vivo*

To characterize the ecological role of the *pks* antibacterial secondary metabolite gene cluster *in vivo*, we gavaged germ-free mice (n=4/group) with a 1:1 mixture of R2lc+100-23, or R2lcΔ*pks*+100-23. To quantify each strain in the fecal material, we engineered R2lc and its derivatives to encode chloramphenicol resistance (R2lc::*Cm* and R2lcΔ*pks*::*Cm*) while strain 100-23 was rifampicin-resistant (100-23—Rif^R). We determined the competition ratio between R2lc and 100-23 (competition ratio: R2lc CFU count/competitor strain's CFU count) over a period of six days in feces. We found that *L. reuteri* R2lc wild-type but not the Δ*pks* mutant gradually outcompetes the 100-23 strain. The R2lc:100-23 competition ratio increased from 107:1 (day 1) up to 980:1 (day 6), while the competition ratio between R2lcΔ*pks*:100-23 declined from 35:1 (day 1) to 4:1 (day 6) (Figure 2A). Similarly, the R2lc:100-23 competition ratio was higher than the R2lcΔ*pks*:100-23 competition ratio in the forestomach (31,973-fold vs 7,8-fold, $P = 0.03$), cecum (1,515-fold vs. 2.9-fold, $P = 0.03$), colon (1,474-fold vs. 8.9-fold, $P = 0.03$) and jejunum (1,114-fold vs. 5.2-fold, $P = 0.03$) (Figure 2B). Thus, our findings demonstrate that Pks provides *L. reuteri* R2lc with a competitive advantage throughout the murine intestinal tract.

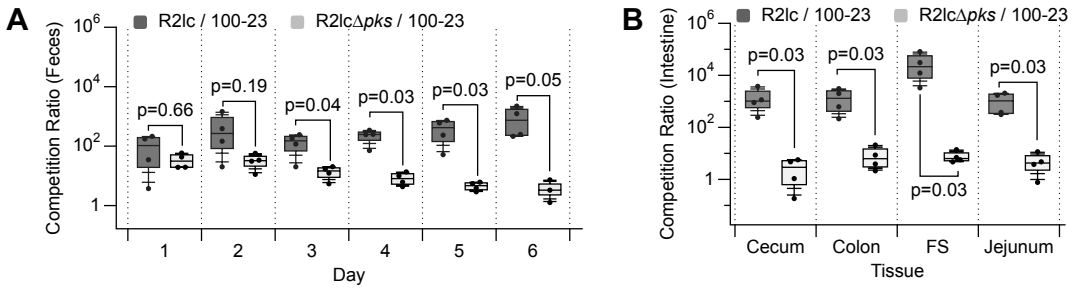

Figure 2. *L. reuteri* Pks molecules provide a competitive advantage *in vivo*.

A 1:1 mixture of R2lc+100-23, or R2lcΔ*pks*+100-23 was administered by oral gavage to germ-free mice. **A)** Competition ratios of the indicated strains in fecal and **B)** intestinal content (day 6) were determined. In box and whisker plots, the whiskers represent the maximum and minimal values, and the lower, middle and upper line of the box represent first quartile, median and third quartile, respectively. Circles represent data from individual mouse. Statistical significance was determined by Wilcoxon / Kruskal-Wallis Tests $p<0.05$ considered as significant. p=P value. F.S.: Forestomach.

L. reuteri Pks-mediated antimicrobial effect is strain specific

Now we established that *L. reuteri* Pks provides an *in vivo* and *in vitro* competitive advantage against strain 100-23, we next investigated to what extent Pks-mediated killing is strain specific. We performed *in vitro* competition experiments with 51 *L. reuteri* gut isolates from different host origins: human, rat, mouse, chicken and pig. To quantify strains, we used derivatives of R2lc and R2lcΔ*pks* that were engineered to be chloramphenicol resistant. For each competitor strain we isolated a natural rifampicin-resistant mutant. Strain R2lc and the competitor strain were mixed 1:1 in MRS medium adjusted to pH 4.0, which is pH of the forestomach, the natural habitat of strain R2lc. The co-cultures were incubated for 24 hours, and appropriate dilutions were plated on MRS plates containing chloramphenicol (5 µg/ml, for R2lc and R2lcΔ*pks*) or rifampicin (25 µg/ml, for competitor strain). Competition ratios were determined after 24 hours of incubation.

Based on non-parametric statistical tests, we identified that R2lc inhibits 41 out of 51 (80.4%) *L. reuteri* strains. Specifically, six out of nine (66.6%) rat-isolates, seven out of ten

(70%) mouse isolates, 16 out of 18 (89%) pig isolates, eight out of nine (88.9%) chicken isolates and two out of five (40%) human isolates were significantly inhibited by R2lc (R2lc vs competitor CFU, $P < 0.05$). To test if the competitive advantage of R2lc is driven by Pks, we repeated the competition experiments with R2lcΔ*pks*. We found that deletion of the *pks* cluster resulted in loss of antimicrobial activity and the Δ*pks* mutant did not show strong inhibition against competitor strains. However, Δ*pks* mutant still inhibited some competitor strains (16 out of 51) to a small extent, with observed differences in Colony Forming Units (CFUs) between Δ*pks* and competitor strains less than two orders of magnitude (Figure 3). These data demonstrate that R2lc-Pks mediated antimicrobial effect is strain specific and 10 out of 51 tested *L. reuteri* strains (19.6%) are not inhibited/outcompeted by the Pks producing strain.

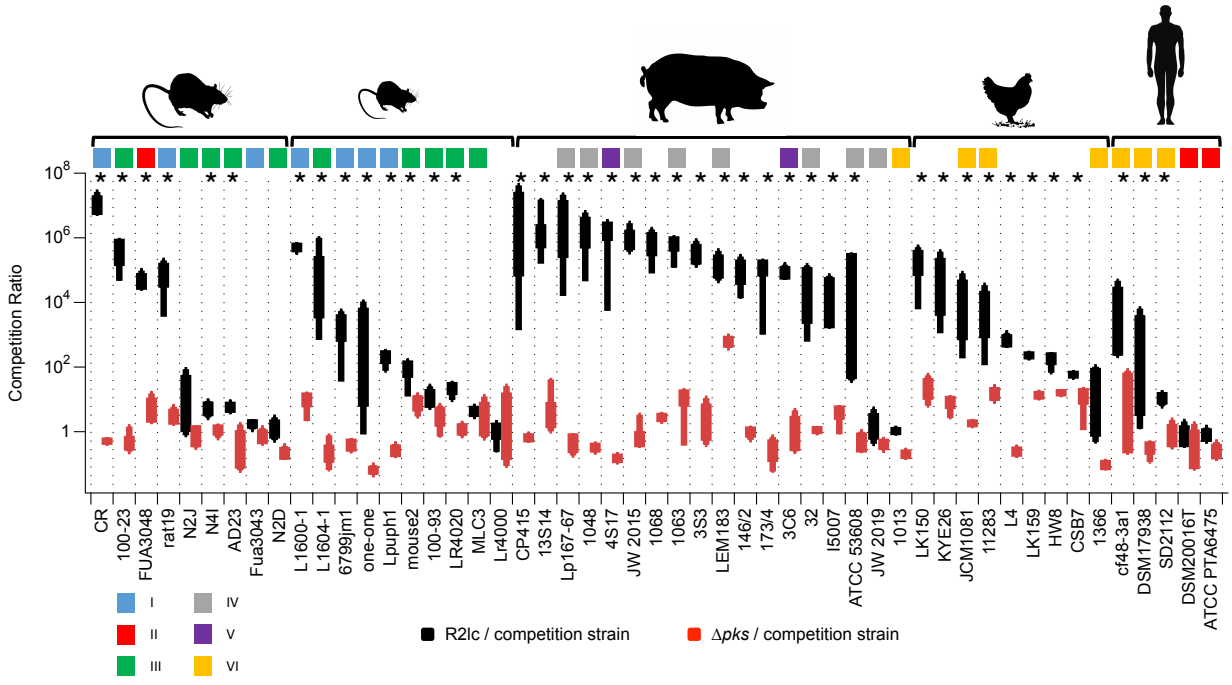

Figure 3. *In vitro* competition ratio of *L. reuteri* R2lc and R2lcΔ*pks* with a panel of 51 *L. reuteri* strains from different host origin. Competition ratios between R2lc and the competitor strain (black) and R2lcΔ*pks* and the competitor strain (red) after 24h co-incubation in MRS (pH 4.0). Data shown are based on at least three biological replicates. The whiskers

represent the maximum and minimal values, and the lower, middle and upper line of the box represent first quartile, median and third quartile, respectively. Host origin (top) and the *L. reuteri* phylogenetic lineage (color coding) are indicated. Statistical significance was determined by Wilcoxon / Kruskal-Wallis Tests. Asterisks (*) represents statistical significance between R2lc vs competitor strain for the top panel ($p<0.05$ considered as significant). See also Table S3.

L. reuteri strains resistant to Pks encode an acyltransferase enzyme

Next, we aimed to understand what the underlying mechanism is that allows select strains to be resistant to *L. reuteri* R2lc Pks. We performed comparative genome analyses to identify genes unique to strains that are resistant to *L. reuteri* R2lc Pks. We included 24 genome sequences in our analyses, of which four genome sequences were derived from resistant strains (mlc3, Lr4000, 6475 and 20016^T) (Table S1). Our initial genome comparison analyses revealed eight genes unique to three of the four R2lc-resistant strains (mlc3, 6475 and 20016^T) (Table S2).

One of the eight unique genes (*act*, Lreu_1368 in strain DSM20016^T, Table S2) is annotated as an O-acyltransferase. This gene became our focus as several studies demonstrated that deletion of homologous *act* genes reduces the resistance to enzymes that target the peptidoglycan cell wall in other Gram-positive bacteria (reviewed in (Ragland and Criss, 2017)). Moreover, resistance to antimicrobial molecules is typically associated with altered cell-wall peptidoglycan structures (Vollmer, 2008). In *L. reuteri*, the *act* gene is located in the surface polysaccharide (SPS) gene cluster. Based on the available genome sequences, we found that three resistant strains (mlc3, 6475 and 20016^T) all putatively encode a nearly identical Act protein (≥99% amino acid identity). Three R2lc-Pks-sensitive strains (CR, ATCC 53608 and one-one) putatively encode a distinct Act protein with 54% amino acid identity to the predicted

243 Act amino acid sequence of resistant *L. reuteri* strains. Six additional R2lc-Pks-sensitive strains
244 (I5007, 6799jm-1, lpup, CF48-3A1, Lr4020 and SD2112) putatively encode Act with 26-28%
245 amino acid identity compared to the predicted Act amino acid sequence of resistant *L. reuteri*
246 strains. The remainder of the 12 strains that are sensitive to R2lc-Pks do not contain the *act* gene
247 in the SPS gene cluster (Figure 4).
248
249
250
251

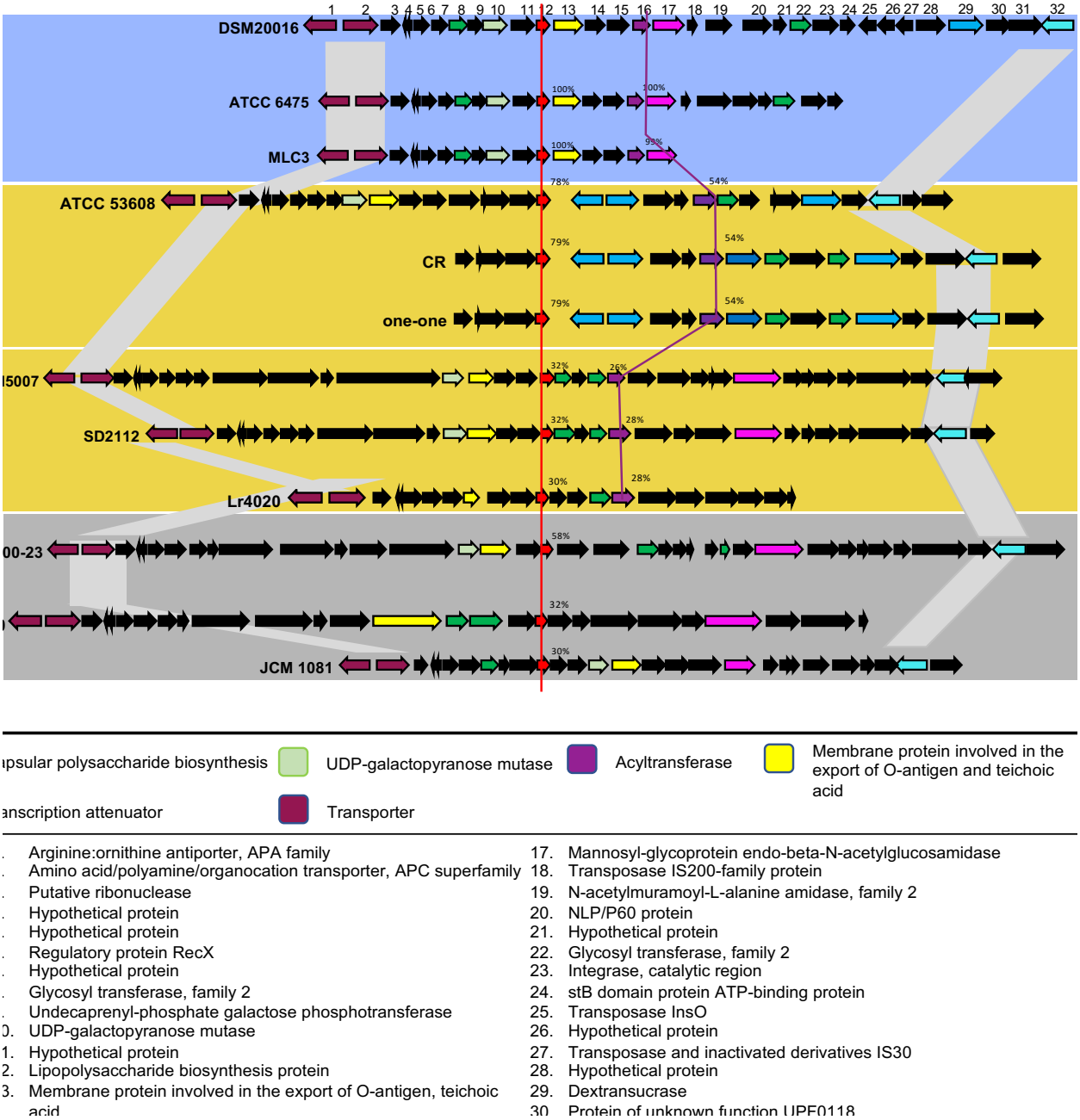

Figure 4. Variability in gene content of Surface Polysaccharide gene cluster in *L. reuteri.*

Comparison of surface polysaccharide (SPS) gene clusters of strains resistant and sensitive to R2lc-Pks. Strains #1-3 (resistant) each putatively encode a nearly identical Act protein with ≥99% amino acid identify; strains #4-6 (sensitive) putatively encode Act that shares 54% amino acid identity to Act of resistant strains; strains #7-9 (sensitive) putatively encode Act that shares

258 25-28% amino acid identity to Act of resistant strains; strains #10-12 (sensitive) lack the *act*
259 gene. Genes are color-coded with their predicted functions based on the annotation of the SPS
260 gene cluster in *L. reuteri* DSM20016^{T}. See also Table S1 and Table S2.

261
262 To map which *L. reuteri* strains are resistant or sensitive to R2lc-Pks, we constructed a
263 phylogenetic tree of Act amino acid sequences from 133 *L. reuteri* strains. We found that 43 out
264 of 133 strains (32.3%) contain an *act* gene whose putative product shares 99-100 amino acid
265 identity to the predicted amino acid sequence of resistant *L. reuteri* strains, while the remaining
266 strains putatively encode Act with 23-72% amino acid identity (Figure 5). Also see Table S6.

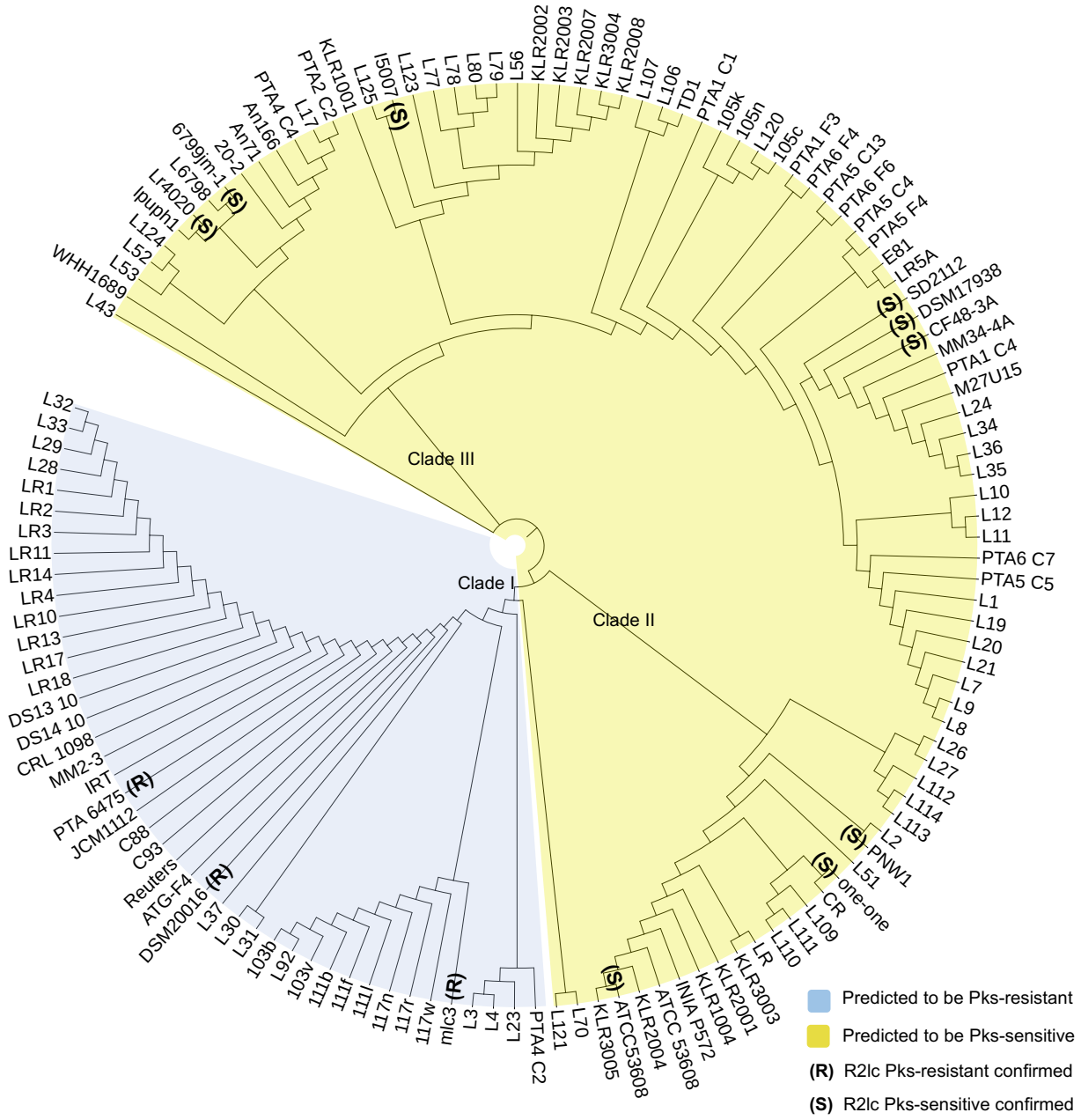

Figure 5. Phylogenetic tree of *L. reuteri* Act homologs. We constructed a phylogenetic tree based on Act amino acid sequences derived from 133 Act encoding *L. reuteri* strains to predict R2lc-resistance and sensitive strains. Fourty-three out of 133 strains (32.3%) encode and *act* gene that shares 99-100 amino acid identify with the *act* gene in ATCC 6475 strain, thus,

predicted to be R2lc-resistant (blue ring). The remaining strains encode an *act* gene that shares 23-54% amino acid identify with the *act* gene in PTA 6475 (yellow ring). See also Table S6.

The acyltransferase gene in *L. reuteri* confers protection to R2lc-Pks products

To test if the *act* gene confers protection to R2lc-Pks products, we generated *act* mutants in three *L. reuteri* strains: mlc3 (rat isolate, clade I), ATCC 6475 (human isolate, clade I), and DSM17938 (human isolate, clade III). In each of these strains, inactivation of *act* increased the sensitivity to R2lc-Pks, as is evident from the increased competition ratios between R2lc *vs* Δ*act* compared to the competition ratios between R2lc *vs* wild-type strain (Figure 6A). In contrast, the competition ratios between R2lcΔ*pks* vs *L. reuteri* Δ*act* strains are across the board lower compared to the competition ratios of R2lc *vs* Δ*act* strains (Figure 6B). Overall, our data showed that the *act* gene in *L. reuteri* confers protection to R2lc-Pks products.

L. reuteri* Act provides resistance against antimicrobial Pks molecules *in vivo

To determine to what extent the *act* gene protects against R2lc Pks *in vivo*, we performed competition experiments in mice. Germ-free mice were administrated with a 1:1 mixture of any of the following strain combinations: R2lc ± *pks* and mlc3 ± *act* (Figure 6BC). Following administration, fecal samples were analyzed at day one, three and six, and animals were sacrificed at day 7 after which we analyzed microbial counts in the stomach, jejunum, cecum and colon. Fecal analyses revealed that the competition ratios between R2lc and mlc3 or its isogenic Δ*act* mutant were comparable ($P > 0.05$); however, at day 7, the competition ratio of R2lc:mlc3Δ*act* was significantly larger compared to R2lc:mlc3 (2,183 ± 3,060-fold *vs* 95 ± 58-fold, respectively; $P < 0.01$). We also observed that in all intestinal tissues the competition ratio of R2lc::mlc3Δ*act* was larger compared to R2lc::mlc3. Specifically, forestomach (3,777 ±

296 2,259-fold *vs* 31 ± 48-fold; $P < 0.01$), jejunum (9,510 ± 15,239-fold *vs* 62 ± 55-fold; $P < 0.01$),
297 cecum (9,872 ± 17,683-fold *vs* 115 ± 99-fold; $P < 0.01$), colon (959 ± 4,703-fold *vs* 118 ±
298 104-fold; $P < 0.01$). Thus, the *act* gene provides protection against R2lc-Pks *in vivo*. To test to
299 what extent R2lc Pks provides R2lc with a competitive advantage in these experiments, we
300 performed competition experiments with R2lcΔ*pks*::mlc3 and R2lcΔ*pks*::mlc3Δ*act* (Figure 6C).
301 Overall, the competition ratios of R2lcΔ*pks*::mlc3 and R2lcΔ*pks*::mlc3Δ*act* are lower compared
302 to the competition ratios observed with R2lc wild-type, which demonstrates a clear role for Pks
303 in providing R2lc with a competitive advantage *in vivo.* Interestingly, the R2lcΔ*pks*::mlc3Δ*act*
304 competition ratio is higher than that of R2lcΔ*pks*::mlc3 in the stomach (1.5-fold vs 0.5-fold, $P =$
305 0.02), jejunum (2.2-fold vs 0.5-fold, $P = 0.01$) and cecum (2.2-fold vs 1.2-fold, $P = 0.04$)
306 (Figure 6C) which might be due to the role of *act* gene in lysozyme resistance during *in vivo*
307 colonization.

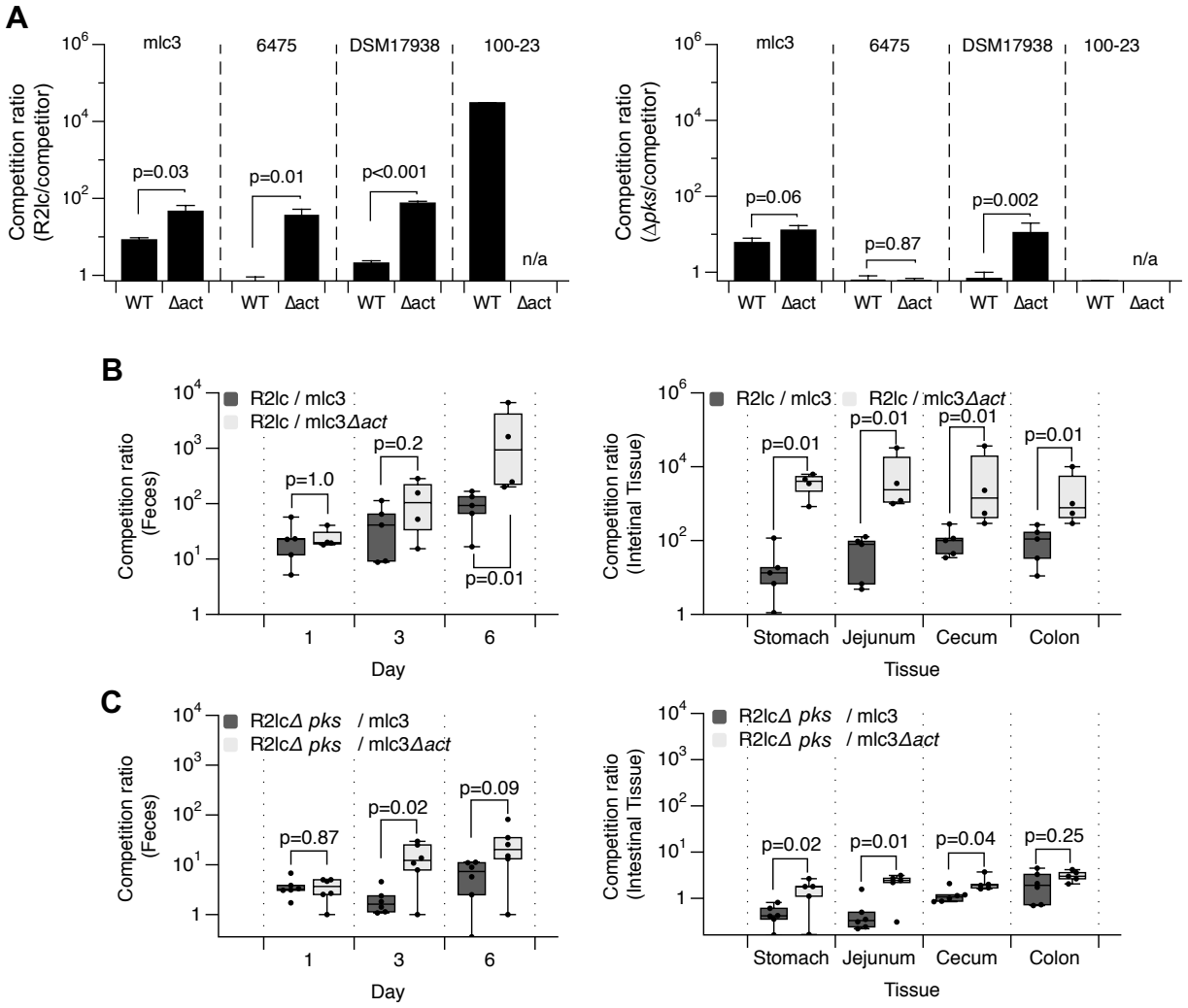

Figure 6. **The *act* acyltransferase gene protects against R2lc-Pks molecules. A)** Act provides resistance to R2lc-mediated killing (left panel), which is mediated by the inhibitory activity of an intact Pks (right panel). **B and C)** Competition ratios of the indicated strains in the previous germ-free mice in fecal (left panel) and intestinal contents (right panels). When data are presented as box and whisker plots, the whiskers represent the maximum and minimal values, and the lower, middle and upper line of the box represent first quartile, median and third quartile, respectively. Points represent individual data points. Statistical significance was determined by Wilcoxon / Kruskal-Wallis Tests, p=P value. P<0.05 considered significant.

The acyltransferase gene increases peptidoglycan acetylation

The bacterial Act enzyme acetylates the C6 hydroxyl of *N*-acylmuramic acid in peptidoglycan (PG) (Moynihan and Clarke, 2010). To understand the role of *act* gene on *L. reuteri* peptidoglycan acetylation, we performed HPLC analyses to determine PG acetylation levels in Pks-resistant and -sensitive strains, relative to total cellular muramic acid (MurN) content. Analysis of cell wall extracts derived from *L. reuteri* 100-23, a Pks-sensitive strain which does not encode Act, revealed that 6.65 ± 1.19% was acetylated relative to total MurN. Next, we cloned the *act* gene from strain mlc3 in the inducible expression vector pSIP411, which was established in strain 100-23. Induced expression of *act* in 100-23 increased the relative peptidoglycan acetylation to 28.7 ± 9.0%. Inactivation of *act* in *L. reuteri* strains resistant to R2lc-Pks reduced peptidoglycan acetylation levels: from 70.1 ± 4.9% to 2.3 ± 0.3% for mlc3; and from 61.2 ± 9.1% to 21.3 ± 12.9% for 6475). Overexpression, of *act* gene in mlc3Δ*act* and 6475Δ*act* restored the relative PG acetylation (from 2.3 ± 0.3% to % to 51.8 ± 15.1% for mlc3Δ*act::act* ; and from 21.3 ± 12.9% to 50.9 ± 9.2% for 6475Δ*act::act*) (Table 1). Together these data suggests that *act* gene in *L. reuteri* is responsible for increased peptidoglycan acetylation, which is linked to the resistance to antimicrobial polyketides produced by R2lc.

Table 1. O-acetylation levels were determined by base-catalyzed hydrolysis and release of acetate. Percent O-acetylation is reported relative to muramic acid (MurN) content.

Strain	% O-acetylation
100-23	6.65 ± 1.19
100-23 + pSIP control	3.46 ± 0.07
100-23::*act*	28.70 ± 9.01
mlc3	70.12 ± 4.85
mlc3Δ*act* + pSIP control	2.31 ± 0.29
mlc3Δ*act*::*act*	51.76 ± 15.09
6475	61.21 ± 9.07
6475Δ*act* + pSIP control	21.29 ± 12.92
6475Δ*act::act*	50.90 ± 9.18

[a] Results are from one representative biological replicate measured in triplicate and reported as mean with Standard Deviation.

Discussion

In this study, we provide mechanistic insight into intra-species antagonism based on a secondary metabolite in the gut symbiont *L. reuteri*. We discovered that a biosynthetic gene cluster (BGC) provides a competitive advantage in the gastrointestinal tract by killing closely related microbes in a strain-specific manner. Expression of the peptidoglycan acetylating enzyme Act by select strains of *L. reuteri* provides protection against this killing activity.

Closely related strains that occupy the same niche are subject to fierce competition (Hibbing et al., 2010). While the co-existence of two closely related strains may be stable in the host, long-term evolution may lead to different ecological outcomes (Edwards et al., 2018). Either evolution leads to changes that form a more stable population—lineages are overall less competitive—or evolution results in increased fitness of one lineage. The lineage with increased fitness will replace the competing lineage, or the competing lineage may evolve in a way that will allow it to persist (Le Gac et al., 2012). Our findings are interesting in light of these ecological theories. Specifically, four distinct lineages have thus far been identified among rodent *L. reuteri* isolates (Frese et al., 2011). Our competition analyses revealed that nearly all strains in lineage I are sensitive to R2lc-Pks products while most strains in lineage III are resistant. One potential explanation for the latter is the broad distribution of nearly identical *act* genes in *L. reuteri* strains from different host origin (Figure 5, blue ring), which suggests *act* exerts an evolutionary pressure that will increase the fitness in the gut ecosystem. The findings presented in this work, the observation that aryl polyene gene clusters are widely distributed throughout the host-associated bacteria (Cimermancic et al., 2014), and that *L. reuteri* 6475Δ*act* has reduced gastrointestinal survival (preliminary data) support the importance of Act in gut

362 fitness and make it collectively less likely that *act* is acquired through a neutral process such as
363 genetic drift.

364 The evolution of a vertebrate symbiont with its host might be reciprocal, resulting in co-
365 evolution. The beneficial traits that a microbe exerts on its host may have been shaped by natural
366 selection as they promote host fitness, which is critical for the microbe to thrive in its niche.
367 R2lc-Pks molecules activates the aryl-hydrocarbon receptor (AhR), a ligand activated
368 transcription factor (Özçam et al., 2019). Activation of AhR has been shown to induce
369 production of interleukin-22 (IL-22) (Veldhoen et al., 2008), which enhances the innate immune
370 response by inducing antimicrobial peptides (i.e. Reg3-lectins) production from the mucosal
371 layer (Vaishnava et al., 2011; Zheng et al., 2008). It is intriguing to speculate that Pks molecules
372 provide R2lc with additional, host-mediated competitive advantage by killing competitors, which
373 may be aided by Pks-mediated AhR activation that leads to antimicrobial peptide production by
374 the host. Collectively, this would support the coevolution between select microbes and their host.

375 This work contributes to our understanding of the ecological role of a gut symbiont-
376 encoded secondary metabolite and provides mechanistic insight into how closely related strains
377 developed resistance against these antimicrobial molecules by acetylation of the cell-wall
378 peptidoglycan. It is plausible bacteria have evolved other mechanisms to survive exposure to
379 Pks. In this work, we did encounter one strain—the rodent isolate Lr4000—that does not encode
380 Act but was resistant to R2lc Pks molecules during the batch culture competition experiments
381 and the mechanism of resistance remains to be elucidated.

382 With a number of genome editing tools available for *L. reuteri*, we are in a position to use
383 genetic approaches to study microbe-microbe interactions in a gut symbiont. When these
384 experiments are placed in the right ecological context, mechanistic insight can be provided on

385 the formation and stability of microbial communities, which is expected to provide insight how
386 microbial diversity is maintained within complex ecosystems. This knowledge can be leveraged
387 to provide rational approaches to select probiotics and next-generation probiotics to ultimately
388 promote animal and human health.

ACKNOWLEDGEMENTS

We thank Siv Ahrné (Lund University, Sweden) for providing *L. reuteri* R2lc, N2J, N2D, and N4I , BioGaia AB (Stockholm, Sweden) for providing *L. reuteri* strains ATCC PTA 6475, and Joseph Skarlupka for technical assistance. We are grateful to the College of Agricultural Life Sciences (CALS) Statistical Consulting Lab for their assistance in the statistical analysis. This work was supported by startup funds from the University of Wisconsin-Madison to J.P.V.P., the UW-Madison Food Research Institute, and the United States Department of Agriculture, National Institute of Food and Agriculture (USDA NIFA) Hatch award MSN185615 and grant no. 2018-6717-27523. M.Ö. received financial support from the Turkish Ministry of National Education, from the Department of Food Science, and is the recipient of the Robert H. and Carol L. Deibel Distinguished Graduate Fellowship in Probiotic Research, which is awarded by the Food Research Institute (UW-Madison). J.C. is supported by National Institutes of Health grant R01 AI153173. Gnotobiotic work was partly supported by the Office of the Vice-Chancellor for Research and Graduate Education at the University of Wisconsin–Madison, with funding from the Wisconsin Alumni Research Foundation.

AUTHOR CONTRIBUTIONS

M.Ö. designed and performed the experiments, analyzed and interpreted the data, and wrote and revised the manuscript. J.-H.O., R.T., D.A., S.Z., C.C., E.V., performed experiments, provided technical support, S.R.R., J.S., performed experiments. T.B., J.C., J.W. shared resources contributed to data interpretation and revised the manuscript; J.P.v.P. secured funding, conceived, designed, and supervised the study, and critically revised the manuscript.

DECLERATION OF INTEREST

JPVP received unrestricted funds from BioGaia, AB, a probiotic-producing company. JPVP is the founder of the consulting company Next-Gen Probiotics, LLC. JW has received grants and honoraria from several food and ingredient companies, including companies that produce probiotics. JW is a co-owner of Synbiotic Solutions, LLC, and is on the Scientific Advisory Board of Alimentary Health. M.Ö. was an employee of DuPont Nutrition and Biosciences. JC is a Scientific Advisor for Seed Health, Inc.

STAR METHODS

RESOURCE AVAILABILITY

Lead contact

Further information and requests for resources should be directed to and will be fulfilled by the Lead Contact, Jan-Peter van Pijkeren (vanpijkeren@wisc.edu).

Material Availability

Requests for the plasmids and strains used in this study should be directed to and will be fulfilled by the Lead Contact, Jan-Peter van Pijkeren (vanpijkeren@wisc.edu).

Data and Code Availability

Any additional information required to reanalyze the data reported in this paper is available from the lead contact upon request.

435

436 **KEY RESOURCE TABLE**

REAGENT or RESOURCE	SOURCE	IDENTIFIER
Bacterial strains		
See Table S3 for bacterial stains used in this study		
Chemicals		
Agar	Alfa	Cat#A10752
Agarose	IBI	Cat# IB70042
LB broth	Acumedia, Neogen	Cat# 7290A
MRS broth	BD	Cat# 288110
M17 broth	BD	Cat# 218561
Potassium Buffered Saline	Gibco	Cat# 14190-144
0.45-µm-pore-size cellulose acetate membrane	Sigma	Product# WHA69012504
Acetic acid standard solution	Fisher Scientific	Cat# A38S-500
Sulfuric acid	Fisher Scientific	Cat# A300-500
Protease	Sigma	Product# P5147
Magnesium sulfate	Fisher Scientific	Cat# M65-500
RNase A	Thermo Scientific	Cat# EN0531
DNase I	Invitrogen	Cat# 18068015
a-amylase	Sigma	Cat# 10065
Sodium cloride	Fisher Scientific	Cat# S271-500
Tris-HCl	Calbiochem	Product# 648310-M
Sodium dodecyl sulfate	Sigma	Product# L4509
24-well plates	Fisher Scientific	Cat# 12556006
Agarose	DOT Scientific Inc.	Cat# DS170042
Pallet paint	VWR International	Cat# 9049-3
Chow diet	LabDiet	Cat# 5201
DpnI	Fisher Scientific	Cat# FERFD1704
0.22 µm filter, Polyvinylidene fluoride [PVDF]	Milipore	Cat# SLGVM33RS
Sodium hydroxide	Fisher Chemical	Cat# S318100
Methanol	Fisher Chemical	Cat# A456-500
Formic acid	Fisher Chemical	Cat# A11350
Chloramphenicol	Dot Scientific	Cat# DSC61000-25
Erythromycin	Fisher Scientific	Cat# BP920-25
Rifampicin	TCI Chemicals	R0079-25G
Vancomycin	Chem-Impex	Cat# 00315
Ethanol	KOPTEC	Cat# V1016
P_{sak} Induction peptide	Peptide2.0	Sequence: MAGNSSNFIHKIKQIFTHR
Choice Taq DNA polymerase master mix	Denville Scientific	Cat# CB4070-8
Phusion Hot Start polymerase II	Thermo Scientific	Cat# F-549-L
T4 DNA ligase	Thermo Scientific	Cat# EL0011
Polynucleotide kinase	Thermo Scientific	Cat# EK0031
dATP	Promega	Cat# U120A
Ampligase	Lucigen	Cat# A32750
Sodium Hydroxide	Fisher Scientific	Cat# S318-500

HCl	Ricca Chemical Company	Cat# 3440-1
Critical Commercial Assay Kits		
Qubit dsDNA quantification kit	Invitrogen	Cat# Q32853
Genomic DNA purification kit	Promega	Cat# A1120
GeneJET PCR purification kit	Thermo Scientific	Cat# K0701
Plasmid isolation kit	Promega	Cat# A9340
Experimental Models: Organisms/Strains		
C57BL/6J, Male	Jackson Laboratory	Cat# 000664
Oligonucleotides		
See Table S4 for primers used for this study		
Recombinant DNA		
See Table S5 for plasmids used for this study		
Software and Algorithms		
JMP Pro	SAS	Ver. 11.0.0
Datagraph	Visual Data Tolls Inc.	Ver. 4.2.1
Bruker Hystar software	Bruker	Hystar 3.2.
MEGA	(Kumar et al., 2018)	Ver. 10.1.7

EXPERIMENTAL MODEL AND SUBJECT DETAILS

Microbial Strains and Growth Conditions

The strains and plasmids used in this study are listed in Table S3 and S5. *L. reuteri* strains were cultured in De Man Rogosa Sharpe (MRS) medium (Difco, BD BioSciences). For *in vitro* competition and biofilm formation experiments, we used filter-sterilized (0.22 µm PVDF filter, Millipore) MRS that was adjusted to pH 4.0 with 1 M HCl. Unless stated otherwise, we prepared bacterial cultures as follows: *L. reuteri* strains were incubated at 37°C under hypoxic conditions (5% CO_2, 2% O_2). The MRS agar plates were incubated for 24 hours for colony counting. *Escherichia coli* EC1000 was used as general cloning host and cultured with aeration at 37°C in lysogeny broth (LB, Teknova). *Lactococcus lactis* MG1363 harboring pJP042 (VPL2047) was cultured under static condition at 30°C in M17 broth, which contains glucose (0.5% [w/v]). Electrocompetent *E. coli* EC1000 were prepared as described in (Sambrook and Russell, 2006). Electrocompetent *L. reuteri* cells were prepared as described in (Van Pijkeren

and Britton, 2012). If applicable, MRS for *L. reuteri* was supplemented with 5 µg/ml erythromycin, 5 µg/ml chloramphenicol or 25 µg/ml rifampicin**.**

Mice

Ethics statement

All mouse experiments were performed in accordance with NIH guidelines, Animal Welfare Act, and US federal law and were approved by the Application Review for Research Oversight at Wisconsin (ARROW) committee and overseen by the Institutional Animal Care and Use Committee (IACUC) under protocol ID M005149-RO1-A01. Conventional pathogen-free and germ-free mice were housed at Animal Science and Laboratory of Animal Research Facilities respectively at the University of Wisconsin-Madison.

Mice Strains and Husbandry

Twelve-week-old germ-free male B6 mice (C57BL/6J) were maintained in a controlled environment in plastic flexible film gnotobiotic isolators with a 12 hours light cycle. Sterilized food (standard chow, LabDiet 5001, St Louis, MO) and water were provided *ad libitum*.

Reagents and Enzymes

To amplify DNA fragments for cloning and screening, we used Phusion Hot Start DNA Polymerase II (Thermo Scientific) and Taq DNA polymerase (Denville Scientific), respectively. We used T4 DNA ligase (Thermo Scientific) for blunt-end ligations. If applicable, we treated column purified (Thermo Scientific) PCR products with DpnI (Thermo Scientific) to remove

474 plasmid template DNA. Phosphorylation of double stranded DNA fragments was performed with
475 T4 Polynucleotide Kinase (Thermo Scientific). Ligase Cycling Reactions (LCR) were performed
476 as described previously (Kok et al., 2014). Oligonucleotides and double-stranded DNA fragments
477 were synthesized by Integrated DNA Technologies (IDT), and are listed in Table S2.
478
479 **METHOD DETAILS**
480
481 **Construction of *L. reuteri* mutant strains**
482 **Construction of suicide shuttle vectors for homologous recombination**
483 To generate mutant strains in lactobacilli we used the counterselection plasmid pVPL3002
484 (Zhang et al., 2018). To generate *L. reuteri* R2lc*::Cm,* R2lcΔ*pks::Cm,* mlc3Δ*act* and
485 DSM17938Δ*act* 500-1000 bp upstream and downstream flanking regions of target genes were
486 amplified by PCR (see Table S4 for oligonucleotides). We used following oligonucleotides;
487 oVPL3113-3114 (upstream, R2lc::*Cm*), oVPL3115-3116 (downstream, R2lc::*Cm*), oVPL3194-
488 3195 (upstream, mlc3Δ*act*), oVPL3196-3197 (downstream, mlc3Δ*act*), oVPL3237-oVPL3238
489 (upstream, DSM17938Δ*act*) and oVPL3239-oVPL3240 (downstream, DSM17938Δ*act*).
490 Amplicons were purified (GeneJET PCR Purification Kit, Thermo Scientific). The
491 pVPL3002 backbone was amplified with oVPL187-oVPL188, purified (GeneJET PCR
492 Purification Kit, Thermo Scientific) and digested with DpnI. Purified amplicons were quantified
493 (Qubit, Life Technologies). The amplicons were mixed at equimolar quantities (0.25 pmol),
494 followed by phosphorylation, ethanol precipitation and LCR (Kok et al., 2014). Following LCR,
495 DNA was precipitated with Pellet Paint co-precipitant (VWR International), resuspended in 5 µl
496 sterile water and transformed into electrocompetent *E. coli* EC1000 cells. By PCR, we screened

for insertion of our target sequences using oligonucleotides that flank the multiple cloning site (oVPL49-oVPL97). Finally, the integrity of deletion and insertion cassettes was determined by Sanger sequencing. The resultant constructs were named as follow; VPL31130 (contains the chloramphenicol insertion cassette for R2lc::*Cm* and R2lcΔ*pks::Cm*), VPL31079 (contains *act* deletion cassette for mlc3) and VPL31139 (contains *act* deletion cassette for DSM17938).

Generating *L. reuteri* mutants by homologous recombination

Three micrograms plasmid DNA was electroporated in electrocompetent *L. reuteri* cells. For R2lc::*Cm,* bacterial cells were plated on MRS agar containing 5 µg/ml chloramphenicol, colonies were screened by PCR (oVPLl3117-3118) to confirm double crossover event. For mlc3Δ*act,* bacterial cells were plated on MRS agar containing 5 µg/ml erythromycin and colonies were screened for single crossover (SCO) event by PCR with oligonucleotide mixtures oVPL3216-oVPL3217-oVPL97 (upstream SCO) and oVPL3216-oVPL3217-oVPL49 (downstream SCO). Following confirmation of SCO, bacterial cells were cultured for one passage in MRS broth without antibiotic selection, and cells were plated on MRS agar plates containing 400 µg/ml vancomycin. For DSM17938Δ*act,* we used a fast-tract liquid-based approach, which does not require isolation of single-crossover recombinants and cells are plated directly on MRS agar plates containing 400 µg/ml vancomycin. Vancomycin-resistant colonies represent cells in which a second homologous recombination event took place (Zhang at al. 2018). To confirm double crossover (DCO), we performed PCR using oligonucleotides oVPL3216-oVPL3217 (for

517 mlc3Δ*act*) and oVPL3244-oVPL3245 (for DSM17938Δ*act*). We used Sanger sequencing to verify
518 the integrity of the recombinant strains.
519
520 **Inactivation of *L. reuteri* 6475 acyltransferase by recombineering**
521 To inactivate the gene putatively encoding acyltransferase (LAR_1287) in *L. reuteri* 6475,
522 we applied single-stranded DNA recombineering using previously established procedure (Van
523 Pijkeren et al., 2012). An 80-mer oligonucleotide identical to the lagging strand with five
524 consecutive mismatches yielded, when incorporated, two in-frame stop codons (Van Pijkeren and
525 Britton, 2012). Electrocompetent *L. reuteri* 6475 cells harboring pJP042 (VPL2047) were
526 transformed with 100 µg oVPL3166. To identify recombinants, we plated cells on MRS plates and
527 recombinant genotypes were identified by mismatch amplification mutation assay (MAMA) PCR
528 (Cha et al., 1992) using oligonucleotide combination oVPL3163-3164-3165. After colony
529 purification, the pure genotype recombinants were confirmed by MAMA-PCR and Sanger
530 sequencing. The resulted mutant strain was named as *L. reuteri* 6475Δ*act.* To cure pJP042, cells
531 were grown in plain MRS for two passages and plated on MRS agar. Then cells were inoculated
532 in MRS containing 5 µg/ml erythromycin to identify cells from which pJP042 was cured.
533
534 **Construction of *L. reuteri* 6475Δ*act::act*, *L. reuteri* 100-23::*act*, and mlc3Δ*act::act***
535 To complement *act* in *L. reuteri* 6475, *L. reuteri* 100-23, and *L. reuteri* mlc3, we cloned
536 the *act* gene from *L. reuteri* 6475 (oVPL3188- oVPL3189) into the pSIP411 backbone (oVPL399-
537 oVPL400). As described above, PCR products were quantified, DpnI treated and LCR reaction
538 was performed with bridging oligonucleotides (oVPL3220-3221) and transformed in *E. coli*
539 EC1000 cells. Insertion was confirmed by colony PCR (oVPL659- oVPL660) and the integrity of

the DNA was confirmed by Sanger sequencing. One microgram of the resulting construct (pVPL31150, hereafter referred to as pSIP-*act*) was transformed in *L. reuteri* 6475Δ*act*, *L. reuteri* 100-23 and *L. reuteri* mlc3Δ*act*. Bacterial cells were plated on MRS agar containing 5 µg/ml erythromycin to identify cells containing pSIP-*act* overexpression plasmid (pVPL31150).

Generating rifampicin resistant *L. reuteri* strains

To enumerate the bacteria co-cultured with R2lc::*cm*, we generated mutants that naturally acquired mutations to yield resistance to rifampicin. Briefly, *L. reuteri* strains were grown in MRS for 16 hours and plated on MRS agar containing 25 µg/ml rifampicin followed by 24 hours of incubation at 37°C under hypoxic condition. Rifampicin resistant colonies were picked from plates and after colony purification stored at -80°C.

Whole Genome Sequencing

Genomic DNA was isolated using the genomic DNA purification kit (Wizard, Promega), and DNA concentrations were determined using the Qubit® (dsDNA High Sensitivity Assay Kit, Life Technologies). Whole genome sequencing was performed at the University of Wisconsin-Madison Biotechnology Center. Samples were prepared according to the Celero PCR Workflow with Enzymatic Fragmentation (NuGEN). Quality and quantity of the finished libraries were assessed using an Agilent bioanalyzer and Qubit® dsDNA HS Assay Kit, respectively. Libraries were standardized to 2 nM. Paired end, 250 bp sequencing was performed using the Illumina NovaSeq6000. Images were analyzed using the standard Illumina Pipeline, version 1.8.2.

Comparative Genome and Bioinformatic Analyses

562 Reads were assembled *de novo* using SPAdes (version 3.11.1) software. Assembled draft
563 genomes were uploaded to National Center of Biotechnology Information (NCBI) (Zhang et al.
564 accepted) and the Joint Genome Institute Integrated Microbial Genomes and Microbes (JGI-IMG)
565 database to perform comparative genome analyses. The web-based comparative genome database
566 Phylogenetic Profiler from the JGI-IMG was used to identify genes present only in *L. reuteri*
567 strains that are resistant to R2lc (ATCC PTA6475 [named as MM4-1A in JGI-IMG], mlc3,
568 DSM20016 and Lr4000).
569 We used *L. reuteri* JCM112 acyltransferase protein sequence (LAR_1287) as a query
570 sequence to search the National Center for Biotechnology Information (NCBI) Nonredundant
571 protein sequence (nr) and JGI-IMG database to identify homologous among *L. reuteri* strains.
572 Partial protein sequences were excluded from the data set. Amino acid sequences of *L. reuteri act*
573 genes were aligned by using MUSCLE (Edgar, 2004), and we constructed the phylogenetic tree
574 with MEGA 7.0 software (Kumar et al. 2016).
575

576 ***In vitro* competition assay with *L. reuteri* strains**

577 *L. reuteri* strains were grown in MRS for 16 hours. The rifampicin resistant competition
578 strains were co-cultured with either R2lc::*Cm* or R2lcΔ*pks::Cm* at optical density OD_{600}: 0.05
579 (from each strain in co-culture) in a pre-warmed MRS broth (pH 4.0). The co-cultures were then
580 incubated for 24 hours at 37°C. After incubation, a serial dilution was performed and 100 µl from
581 appropriate dilution was plated to MRS plates containing chloramphenicol (5 µg/ml) or rifampicin
582 (25 µg/ml). After 24 hours of incubation, we determined the competition ratios.
583

584 ***In vitro* biofilm assay**

585 *L. reuteri* R2lc, R2lcΔ*pks* and 100-23 cultures were inoculated into 2 ml MRS broth at
586 OD_{600}= 0.1 (0.05 from each strain if co-culture) in 24-well plates (Fisher Scientific) and incubated
587 for 24 hours. The culture supernatant was removed and bacterial biofilm was washed three times
588 with 1 ml PBS. The adherent cells were scraped from the well and re-suspended in 2 ml PBS.
589 For colony enumeration, the suspended cultures were plated on MRS plates containing
590 chloramphenicol (5 µg/ml) for R2lc and R2lcΔ*pks* or rifampicin (25 µg/ml) for 100-23, and
591 incubated for 24 hours.
592
593 ***In vivo* competition experiment**
594 Germ-free B6 (C57BL/6J, male 12-week old, n=4-5mice/group) mice were maintained in
595 sterile biocontainment cages in the gnotobiotic animal facility at the University of Wisconsin-
596 Madison. Mice were colonized following a single oral gavage of 200 µl *L. reuteri* cocktail in
597 PBS (1:1 ratio, ~2×10^8 CFU). Each group was gavaged with a mixture of either *L. reuteri*
598 R2lc::*Cm* + competition strain or *L. reuteri* R2lcΔ*pks::Cm* + competition strain. Twenty-four
599 hours following colonization, fecal samples were collected daily from individual mice to
600 determine the fecal CFUs. Fecal samples were homogenized and diluted in PBS followed by
601 plating on MRS-Cm and MRS-Rif. After 24 hours of incubation colonies were counted. At day
602 7, mice were sacrificed by CO_2 asphyxiation and digesta from forestomach, jejunum, cecum and
603 colon were collected, weighed and re-suspended with PBS (100 mg/ml) to determine the CFUs
604 per 100 mg content.
605
606 **Determination of peptidoglycan O'-acylation by HPLC**

Peptidoglycan (PG) was extracted following a previously reported method (Ha et al., 2016) with some modifications. After 16 hours of incubation, the cells were harvested by centrifugation at 5,000 × *g* and 4 °C for 5 min, washed twice with 10 mM sodium phosphate buffer (pH 6.5) and then resuspended in 50 ml of water (pH 5.5 to 6.0). The cell suspension was boiled in an equal volume of 8% (w/v) sodium dodecyl sulfate (SDS, 4% w/v final concentration) in 25 mM SP buffer (pH 6.5) for 1 hour under reflux with stirring. Samples were centrifuged (30,000 × *g*) and the SDS-insoluble PG was washed (5 times) with sterile double distilled H_2O to completely remove SDS and lyophilized. Lyophilized PG was dissolved in 4 ml of 1:1 mixture of 10 mM Tris-HCl (pH 6.5) and 10 mM NaCl and sonicated for 2 min. The PG suspension was treated with 100 µg/ml α-amylase (from *Bacillus sp*., Sigma), 10 µg/ml DNase I (Invitrogen), 50 µg/ml RNase A (Thermo Scientific), and 20 mM $MgSO_4$ solution and incubated overnight at 37 °C with shaking. The PG suspension was further treated with 200 µg/ml protease (from *Streptomyces griseus*, Sigma) and incubated overnight at 37 °C with shaking. Samples were then re-extracted by boiling in 1% SDS for 40 min, washed, lyophilized and stored at -20 °C until use.

For the analysis of acetate release from PG, lyophilized PG (20 mg) was dissolved in 150 µl ddH_2O and mixed with an equal volume of either 160 mM NaOH or 160 mM sodium phosphate buffer (pH 6.5) and incubated overnight at 37°C with shaking. The peptidoglycan was collected by centrifugation at 15,000 × *g* for 20 min. The supernatant was filtered through a 0.45-µm-pore-size cellulose acetate membrane and quantitation of released acetate was carried out in a Dionex UltiMate 3000 HPLC equipped with an LPG-3400 quaternary pump, a WPS-3000 analytical autosampler, and a DAD-3000 diode array detector. The filtered supernatants or 100 µM of acetic acid standard solution were injected onto a 300 × 7.8 mm Rezex™ ROA-Organic

629 Acid H^+ (8%) column and eluted isocratically with 20 mM H_2SO_4 at 0.5 ml min^{-1}. The column
630 was maintained and 40 °C and absorbance was monitored at 210 nm.
631
632 **LC/MS Sample preparation**
633 An aliquot of 1.5 ml from each of the cultures were collected in Eppendorf tubes and
634 centrifuged at 2152 × *g* for 5 min. The supernatants were collected and transferred to dram vials
635 and the cell pellets were incubated for 1 hour in 100 µl methanol. Next, the samples were
636 centrifuged again and the methanol extracts were added to 1 dram vials. A Gilson GX-271 liquid
637 handling system was used to subject 900 µL of the samples to automated solid phase extraction
638 (SPE). Extracts were loaded onto pre-conditioned (1 ml MeOH followed by 1 ml H_2O) EVOLUTE
639 ABN SPE cartridges (25 mg absorbent mass, 1 ml reservoir volume; Biotage, S4 Charlotte, NC).
640 Samples were subsequently washed using H_2O (1 ml) to remove media components, and eluted
641 with MeOH (500 µL) directly into an LC/MS-certified vial.
642
643 **UHPLC/HRESI-qTOF-MS Analysis of Extracts**
644 LC/MS data were acquired using a Bruker MaXis ESI-qTOF mass spectrometer (Bruker,
645 Billerica, MA) coupled with a Waters Acquity UPLC system (Waters, Milford, MA) with a PDA
646 detector operated by Bruker Hystar software, as previously described (Hou et al., 2012). Briefly,
647 a solvent system of MeOH and H_2O (containing 0.1% formic acid) was used on an RP C-18 column
648 (Phenomenex Kinetex 2.6µm, 2.1 × 100 mm; Phenomenex, Torrance, CA) at a flow rate of 0.3
649 ml/min. The chromatogram method started with a linear gradient from MeOH/ H_2O (10%/90%)
650 to MeOH/ H_2O (97%/3%) in 12 min, then held for 2 min at MeOH/ H_2O (97%/3%). Full scan mass
651 spectra (m/z-150-1550) were measured in positive Electrospray Ionization (ESI) mode. The mass

652 spectrometer was operated using the following parameters: capillary, 4.5 kV; nebulizer pressure,
653 1.2 bar; dry gas flow, 8.0 L/min; dry gas temperature, 205 °C; scan rate, 2 Hz. Tune mix (ESI-L
654 low concentration; Agilent, Santa Clara, CA) was introduced through a divert valve at the end of
655 each chromatographic run for automated internal calibration. Bruker Data Analysis 4.2 software
656 was used for analysis of chromatograms.
657
658
659

SUPPLEMENTARY FIGURES

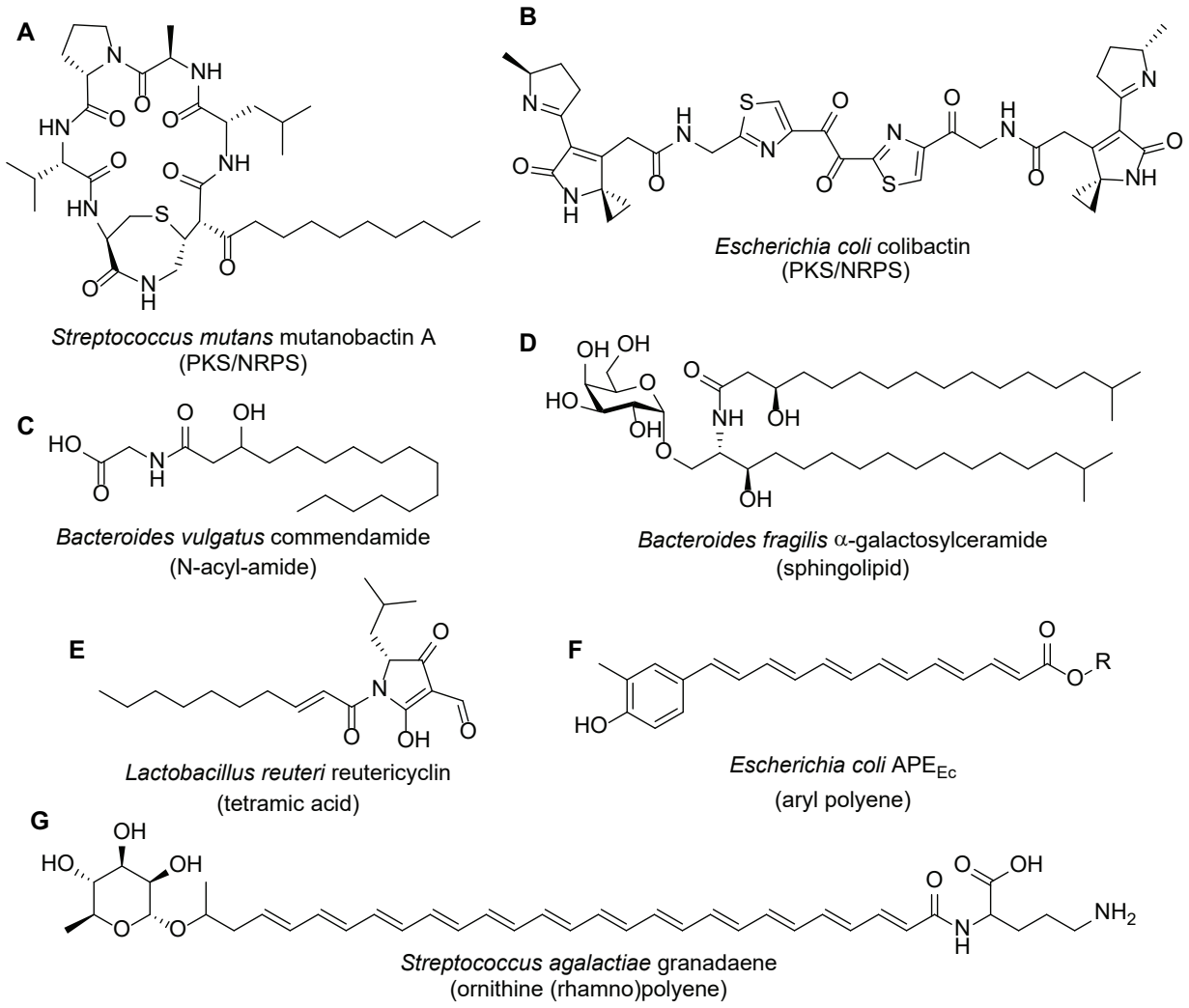

Figure s1. Structures of bioactive fatty acid-like, polyketide and NRPS/PKS hybrid compounds in bacteria from the gastrointestinal tract. Up to date, there are only seven microbial metabolites from GI tract have been chemically identified. These are an antifungal PKS/NRPS hybrid metabolite, Mutanobactin A produced by *Steptococcus mutans,* a genotoxin PKS/NRPS hybrid metabolite, Colibactin produced by *Escherichia coli*; a G-Protein Coupled Receptors (GPCR) agonist N-acyl-amide metabolite, Mutanobactin A, produced by *Bacteroides vulgatus*; an invariant Natural Killer Cell (iNTK) activator sphingolipid metabolite, α-

669 galactosylceramide, produced by *Bacteroides fragilis*; an antimicrobial tetramic acid metabolite,
670 Reutericyclin, produced by *Lactobacillus reuteri*; an antioxidant aryl polyene molecule, APEEC,
671 produced by *Escherichia coli*; a polyene ornithine compound, Granadaene, produced by
672 *Streptococcus agalactiae*. Related to Introduction.
673

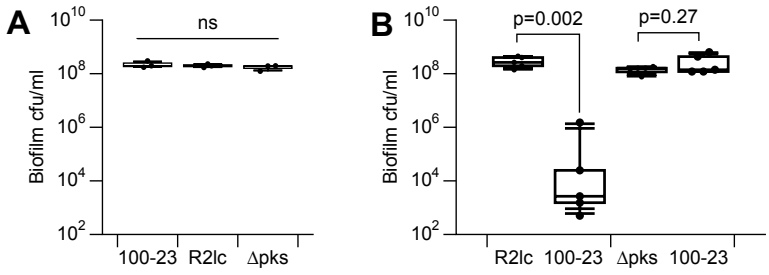

674

675 **Figure s2. A polyketide synthase cluster in *L. reuteri* R2lc inhibits biofim formation of *L.***
676 ***reuteri* 100-23. A)** Quantification of the number of CFU in single and **B)** co-culture biofilm. For
677 box and whisker plots, the whiskers represent the maximum and minimal values, and the lower,
678 middle and upper line of the box represent first quartile, median and third quartile, respectively.
679 Circles represent individual data points. All data represent an average of at least three
680 independent experiments. Statistical significance was determined by Wilcoxon / Kruskal-Wallis
681 Tests $p<0.05$ considered as significant. p=P value. Related to Figure 1.
682

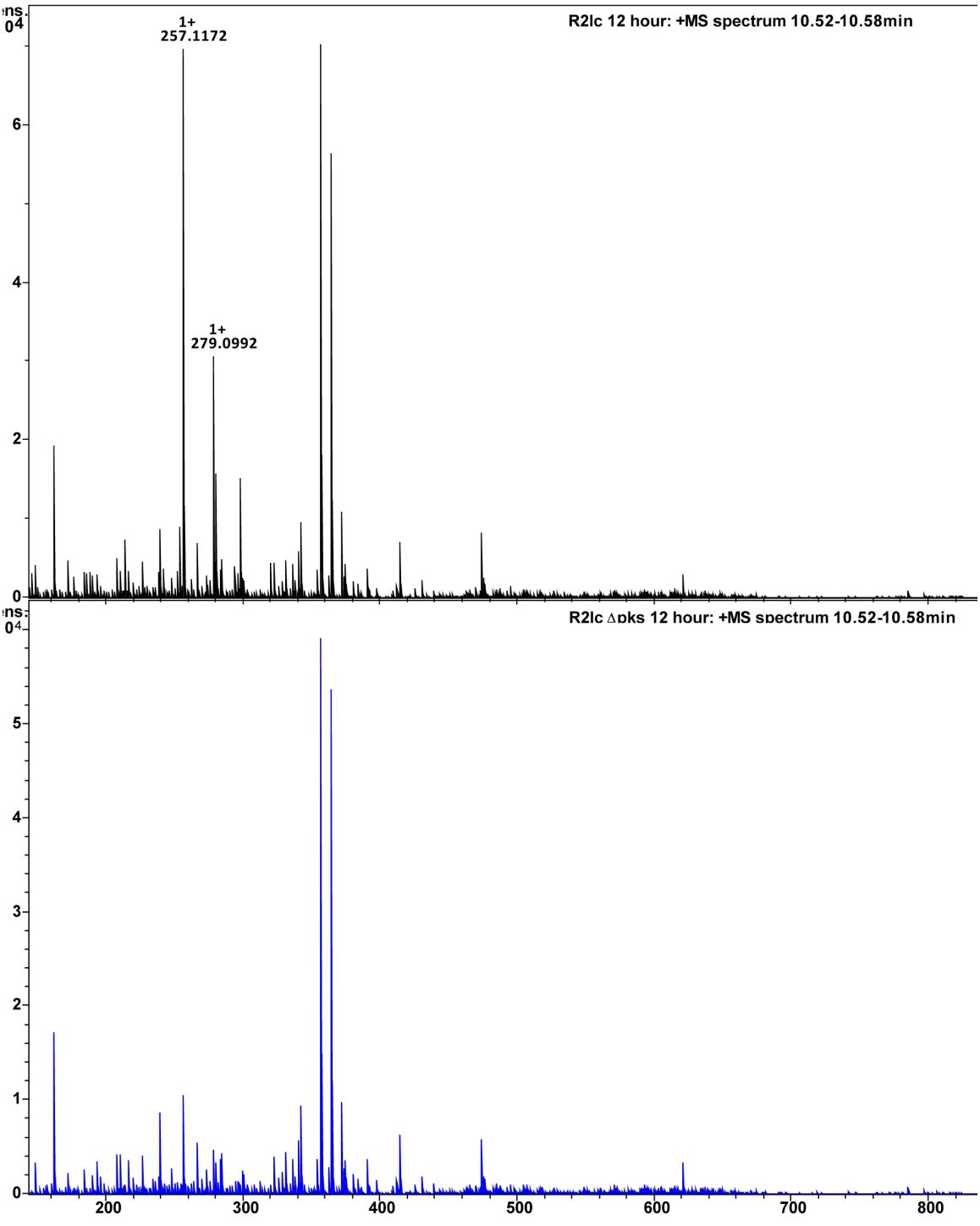

683

684 **Figure s3. R2lc but not *pks* mutant produces unique compounds.** The mass spectrum of the

685 peak between 10.52 min –10.58 min in the R2lc chromatogram at 12 hours clearly showed an ion

686 with m/zvalue of 257.1172 as the [M+H]+and 279.0092 as the corresponding [M+Na]+ which

were absent in the corresponding 12-hour culture of Δpks. Bruker Smart Formula algorithm, which uses both the exact mass of the molecular ion and the isotopic pattern allowed accurate determination of the molecular formula as $C_{16}H_{16}O_3$. Related to Figure 1.

Table S1. Strains used for comparative genome analyses.

Strain Number	Strain	Sensitive/Resistant*
1	CR	S
2	100-23	S
3	L1604-1	S
4	ATCC53608	S
5	3c6	S
6	L1600-1	S
7	one-one	S
8	rat19	S
9	JCM1081	S
10	I5007	S
11	6799jm-1	S
12	lpuph	S
13	CF48-3A1	S
14	1366	S
15	N2J	S
16	LR4020	S
17	SD2112	S
18	AD23	S
19	N4I	S
20	100-93	S
21	PTA6475	R
22	DSM20016^T	R
23	mlc3	R
24	Lr4000	R

*Sensitive/resistant phenotypes were determined based on statistical analyses shown in Figure 4. S: sensitive, R: Resistant. Related to Figure 4.

Table S2. Unique genes in R2lc-resistat 6475, DSM20016^T and mlc3.

Locus Tag	Gene Name	Length (aa)
Lreu_0435	hypothetical protein	69
Lreu_0848	holin, Cph1 family	149
Lreu_1143	transcription regulator, XRE family	67
Lreu_1353	hypothetical protein	522
Lreu_1362	glycosyltransferase	324
Lreu_1368	acyltransferase	355
Lreu_1869	hypothetical protein	175

aa: amino acid. Related to Figure 4.

Table S3. Bacterial strains used in this study.

Genus and Species	**Strain**	**VPL identifier**	**Description/ Origin**	**Source**
Escherichia coli	EC1000	VPL1009	Cloning host	(Leenhouts et al., 1996)
Lactococcus lactis ssp. cremoris	MG1363	VPL2005	*L. lactis* MG1363 harboring pSIP411	Laboratory stock
Lactobacillus reuteri	R2lc	VPL1053	Rat	Siv Ahrné—JGI 2716884882
Lactobacillus reuteri	R2lc::*Cm*	VPL4231	Insertion of *Cm* gene in R2lc chromosome	This study
Lactobacillus reuteri	R2lcΔ*fun::Cm*	VPL4234	Insertion of *Cm* gene in R2lcΔ*fun* chromosome	This study
Lactobacillus reuteri	R2lcΔ*pks::Cm*	VPL4209	Insertion of *Cm* gene in R2lcΔ*pks* chromosome	(Özçam et al., 2019)
Lactobacillus reuteri	6475 (pJP042)	VPL2047	6475 harboring pJP042 plasmid	(Van Pijkeren and Britton, 2012)
Lactobacillus reuteri	6475Δ*act*	VPL4241	Deletion of act gene in 6475	This study
Lactobacillus reuteri	6475Δ*act*—Rif^R (pSIP411)	VPL31153	6475Δ*act*—Rif^R harboring pSIP411 plasmid	This study
Lactobacillus reuteri	6475Δ*act::act*—Rif^R	VPL4250	6475Δ*act*—Rif^R harboring pSIP-*act* plasmid	This study
Lactobacillus reuteri	100-23	VPL1049	Rat	JGI: 2500069000
Lactobacillus reuteri	100-23—Rif^R	VPL4251	100-23 Rif resistant	This study
Lactobacillus reuteri	100-23—Rif^R (pSIP411)	VPL31155	100-23—Rif^R harboring pSIP411 plasmid	This study
Lactobacillus reuteri	100-23::*act*—Rif^R	VPL4249	Deletion of act gene in 100-23, Rif resistant	This study
Lactobacillus reuteri	6475	VPL1014	Human	BioGaia AB
Lactobacillus reuteri	6475—Rif^R	VPL4296	6475, Rif resistant	This study
Lactobacillus reuteri	SD2112	VPL1013	Human	BioGaia AB
Lactobacillus reuteri	SD2112—Rif^R	VPL4297	SD2112, Rif resistant	This study
Lactobacillus reuteri	CSB7	VPL1168	Chicken	Jens Walter
Lactobacillus reuteri	CSB7—Rif^R	VPL4298	CSB7, Rif resistant	This study
Lactobacillus reuteri	KYE26	VPL1162	Chicken	Jens Walter
Lactobacillus reuteri	KYE26—Rif^R	VPL4299	KYE26, Rif resistant	This study
Lactobacillus reuteri	LK159	VPL1156	Chicken	Jens Walter
Lactobacillus reuteri	LK159—Rif^R	VPL4301	LK159, Rif resistant	This study
Lactobacillus reuteri	L4	VPL1173	Chicken	Jens Walter
Lactobacillus reuteri	L4—Rif^R	VPL4302	L4, Rif resistant	This study
Lactobacillus reuteri	mouse2	VPL1070	Mouse	(Frese et al., 2011)
Lactobacillus reuteri	Mouse2—Rif^R	VPL4252	Mouse2, Rif resistant	This study
Lactobacillus reuteri	N2J	VPL1052	Rat	(Frese *et al*. 2011)
Lactobacillus reuteri	N2J—Rif^R	VPL4253	N2J, Rif resistant	This study
Lactobacillus reuteri	one-one	VPL1060	Mouse	(Frese *et al*. 2011)
Lactobacillus reuteri	one-one—Rif^R	VPL4254	one-one, Rif resistant	This study
Lactobacillus reuteri	ATCC 53608	VPL1090	Pig	BioGaia AB EMBL LN906634
Lactobacillus reuteri	ATCC 53608—Rif^R	VPL4255	ATCC 53608, Rif resistant	This study

Lactobacillus reuteri	L1600-1	VPL1064	Mouse	(Frese *et al*. 2011)
Lactobacillus reuteri	L1600-1—Rif^R	VPL4256	L1600-1, Rif resistant	This study
Lactobacillus reuteri	N2D	VPL1067	Rat	Siv Ahrné
Lactobacillus reuteri	N2D—Rif^R	VPL4257	N2D, Rif resistant	This study
Lactobacillus reuteri	DSM17938	VPL4171	Human	BioGaia AB
Lactobacillus reuteri	DSM17938—Rif^R	VPL4258	DSM17938, Rif resistant	This study
Lactobacillus reuteri	DSM17938Δ*act*	VPL4313	Deletion of *act* gene in DSM17938	This study
Lactobacillus reuteri	DSM17938Δ*act*—Rif^R	VPL4315	DSM17938Δ*act*, Rif resistant	This study
Lactobacillus reuteri	Lr4000	VPL1071	Mouse	BioGaia AB
Lactobacillus reuteri	Lr4000—Rif^R	VPL4259	Lr4000, Rif resistant	This study
Lactobacillus reuteri	CF48-3A1	VPL1086	Human	BioGaia AB—JGI2502171173
Lactobacillus reuteri	CF48-3A1—Rif^R	VPL4260	CF48-3A1, Rif resistant	This study
Lactobacillus reuteri	L1604-1	VPL1066	Mouse	(Frese *et al*. 2011)
Lactobacillus reuteri	L1604-1—Rif^R	VPL4261	L1604-1, Rif resistant	This study
Lactobacillus reuteri	CR	VPL1059	Rat	(Frese *et al*. 2011)
Lactobacillus reuteri	CR—Rif^R	VPL4262	CR, Rif resistant	This study
Lactobacillus reuteri	mlc3	VPL1050	Mouse	JGI: 2506381016
Lactobacillus reuteri	mlc3—Rif^R	VPL4263	mlc3, Rif resistant	JGI: 2506381016
Lactobacillus reuteri	mlc3Δ*act*	VPL4246	Deletion of *act* gene in mlc3	This study
Lactobacillus reuteri	mlc3Δ*act*—Rif^R	VPL4308	mlc3Δ*act*, Rif resistant	This study
Lactobacillus reuteri	mlc3Δ*act*—Rif^R (pSIP411)	VPL31177	mlc3Δ*act*—Rif^R, harboring pSIP411 plasmid	This study
Lactobacillus reuteri	mlc3Δ*act::act*—Rif^R	VPL31165	mlc3Δ*act*—Rif^R harboring pSIP-*act* plasmid	This study
Lactobacillus reuteri	I5007	VPL1082	Pig	JGI: 2554235423
Lactobacillus reuteri	I5007—Rif^R	VPL4264	I5007, Rif resistant	This study
Lactobacillus reuteri	Lr4020	VPL1072	Mouse	(Frese *et al*. 2011)
Lactobacillus reuteri	Lr4020—Rif^R	VPL4265	Lr4020, Rif resistant	This study
Lactobacillus reuteri	Lp167-67	VPL1085	Pig	BioGaia AB JGI 2599185361
Lactobacillus reuteri	Lp167-67—Rif^R	VPL4266	Lp167-67, Rif resistant	This study
Lactobacillus reuteri	N4I	VPL1063	Rat	(Frese *et al*. 2011)
Lactobacillus reuteri	N4I—Rif^R	VPL4267	N4I, Rif resistant	This study
Lactobacillus reuteri	3c6	VPL1083	Pig	JGI: 2599185333
Lactobacillus reuteri	3c6—Rif^R	VPL4268	3c6, Rif resistant	This study
Lactobacillus reuteri	FUA3043	VPL1062	Rat	(Frese *et al*. 2011)
Lactobacillus reuteri	FUA3043—Rif^R	VPL4269	FUA3043, Rif resistant	This study
Lactobacillus reuteri	Rat 19	VPL1069	Rat	(Frese *et al*. 2011)
Lactobacillus reuteri	Rat 19—Rif^R	VPL4270	Rat 19, Rif resistant	This study
Lactobacillus reuteri	6799jm-1	VPL1051	Mouse	(Frese *et al*. 2011)
Lactobacillus reuteri	6799jm-1—Rif^R	VPL4271	6799jm-1, Rif resistant	This study
Lactobacillus reuteri	100-93	VPL1047	Mouse	(Frese *et al*. 2011)
Lactobacillus reuteri	100-93—Rif^R	VPL4272	100-93, Rif resistant	This study
Lactobacillus reuteri	Lpuph-1	VPL1056	Mouse	JGI: 2506381017
Lactobacillus reuteri	Lpuph-1—Rif^R	VPL4273	Lpuph-1, Rif resistant	This study
Lactobacillus reuteri	DSM 20016	VPL1046	Human	JGI: 640427118

Lactobacillus reuteri	DSM 20016—Rif^R	VPL4274	DSM 20016, Rif resistant	This study
Lactobacillus reuteri	AD 23	VPL1048	Rat	(Frese *et al*. 2011)
Lactobacillus reuteri	AD 23—Rif^R	VPL4275	AD 23, Rif resistant	This study
Lactobacillus reuteri	173/4	VPL1135	Pig	Jens Walter
Lactobacillus reuteri	173/4—Rif^R	VPL4276	173/4, Rif resistant	This study
Lactobacillus reuteri	4S17	VPL1122	Pig	(Frese *et al*. 2011)
Lactobacillus reuteri	4S17—Rif^R	VPL4277	4S17, Rif resistant	This study
Lactobacillus reuteri	1366	VPL1115	Chicken	Jens Walter
Lactobacillus reuteri	1366—Rif^R	VPL4278	1366, Rif resistant	This study
Lactobacillus reuteri	JW2015	VPL1126	Pig	Jens Walter
Lactobacillus reuteri	JW2015—Rif^R	VPL4279	JW2015, Rif resistant	This study
Lactobacillus reuteri	32	VPL1137	Pig	Jens Walter
Lactobacillus reuteri	32—Rif^R	VPL4280	32, Rif resistant	This study
Lactobacillus reuteri	3S3	VPL1120	Pig	Jens Walter
Lactobacillus reuteri	3S3—Rif^R	VPL4281	3S3, Rif resistant	This study
Lactobacillus reuteri	13S14	VPL1118	Pig	Jens Walter
Lactobacillus reuteri	13S14—Rif^R	VPL4282	13S14, Rif resistant	This study
Lactobacillus reuteri	LK150	VPL1112	Chicken	Jens Walter
Lactobacillus reuteri	LK150—Rif^R	VPL4283	LK150, Rif resistant	This study
Lactobacillus reuteri	JCM 1081	VPL1110	Chicken	Jens Walter
Lactobacillus reuteri	JCM 1081—Rif^R	VPL4284	JCM 1081, Rif resistant	This study
Lactobacillus reuteri	HW8	VPL1166	Chicken	Jens Walter
Lactobacillus reuteri	HW8—Rif^R	VPL4300	HW8, Rif resistant	This study
Lactobacillus reuteri	JW2019	VPL1129	Pig	Jens Walter
Lactobacillus reuteri	JW2019—Rif^R	VPL4286	JW2019, Rif resistant	This study
Lactobacillus reuteri	1133 (146/2)	VPL1133	Pig	Jens Walter
Lactobacillus reuteri	1133 (146/2)—Rif^R	VPL4287	1133, Rif resistant	This study
Lactobacillus reuteri	CP415	VPL1146	Pig	Jens Walter
Lactobacillus reuteri	CP415—Rif^R	VPL4288	CP415, Rif resistant	This study
Lactobacillus reuteri	1063	VPL1143	Pig	Jens Walter
Lactobacillus reuteri	1063—Rif^R	VPL4289	1063, Rif resistant	This study
Lactobacillus reuteri	1068	VPL1142	Pig	Jens Walter
Lactobacillus reuteri	1068—Rif^R	VPL4291	1068, Rif resistant	This study
Lactobacillus reuteri	1048	VPL1141	Pig	Jens Walter
Lactobacillus reuteri	1048—Rif^R	VPL4292	1048, Rif resistant	This study
Lactobacillus reuteri	1013	VPL1140	Pig	Jens Walter
Lactobacillus reuteri	1013—Rif^R	VPL4293	1013, Rif resistant	This study
Lactobacillus reuteri	1704	VPL1139	Pig	Jens Walter
Lactobacillus reuteri	1704—Rif^R	VPL4294	1704, Rif resistant	This study
Lactobacillus reuteri	FUA3048	VPL1063	Rat	(Frese *et al*. 2011)
Lactobacillus reuteri	FUA3048 —Rif^R	VPL4295	FUA3048, Rif resistant	This study

VPL: Van Pijkeren Laboratory strain identification number. pVPL: Van Pijkeren Laboratory plasmid identification number. Rif^R: rifampicin-resistant; *act*: acyltransferase; JGI: Joint Genome Institute; Cm: Chloramphenicol; Rif: Rifampicin.

Table S4. Oligonucleotides used in this study.

Oligonucleotide	**Sequence (5'-3')**	**Target/Comment**
oVPL49	acaatttcacacaggaaacagc	F. Insert screening of pVPL3002.
oVPL97	cccccattaagtgccgagtgc	R. Insert screening of pVPL3002.

oVPL187	taccgagctcgaattcactgg	R. amplifies pVPL3002 backbone.
oVPL188	atcctctagagtcgacctgc	F. amplifies pVPL3002 backbone.
oVPL3113	acgcacgacaggaagaatttg	F. amplifies u/s flanking region of CmR^+ insertion cassette.
oVPL3114	agactcgagccttgtggc	R. amplifies u/s flanking region of CmR^+ insertion cassette
oVPL3115	aagtacgaacgataatcagccc	F. amplifies d/s flanking region of CmR^+ insertion cassette.
oVPL3116	agccagtattatgacgggtc	R. amplifies d/s flanking region of CmR^+ insertion cassette
oVPL2856	agtgtcatggcgcattaacg	F. amplifies CmR^+ gene.
oVPL2857	ttataaaagccagtcattaggcc	R. amplifies CmR^+ gene
oVPL3166	tattaatgttattactagcaaacgaattaataaaatcctattaactag gattaggatgcaacgatggaccaggataagca	*L. reuteri* 6475 *act* gene recombineering oligo.
oVPL3163	tgaacaaattcaggccaattatctgg	F. screening *act* gene
oVPL3164	tgtagttgtttggcgtcaggc	R. screening *act* gene
oVPL3165	cgttgcatcctaatcctagttaatag	MAMA oligonucleotide for *act* gene
oVPL659	tgccccgttagttgaagaag	F. amplifies pSIP411 backbone.
oVPL660	attctgctcccgcccttatg	R. amplifies pSIP411 backbone.
oVPL3188	ttaaggaattatcatcctaacaaatttattc	F. amplifies *act* gene in *L. reuteri* 6475.
oVPL3189	atgcttaatagtaagagactccac	R. amplifies *act* gene in *L. reuteri* 6475.
oVPL3194	acgatattgaatctttgcgactcc	F. amplifies u/s flanking region of *act* gene in *L. reuteri* mlc3.
oVPL3195	tagtggagtctcttactattaag	R. amplifies u/s flanking region of *act* gene in *L. reuteri* mlc3.
oVPL3196	aggaatattgtctggagtaagc	F. amplifies d/s flanking region of *act* gene in *L. reuteri* mlc3.
oVPL3197	ccattgtgactgtacatagtt	R. amplifies d/s flanking region of *act* gene in *L. reuteri* mlc3.
oVPL3198	aaacgacggccagtgaattcgagctcggtaacgatattgaatctt tgcgactccattatg	LCR bridging oligonucleotide to ligate plasmid backbone + u/s flanking region of mlc3Δ*act* deletion cassette.
oVPL3199	aattatgcttaatagtaagagactccactaaggaatattgtctgga gtaagcttaggaat	LCR bridging oligonucleotide to ligate u/s + d/s flanking region of mlc3Δ*act* deletion cassette.
oVPL3200	gtagataataactatgtacagtcacaatggatcctctagagtcga cctgcaggcatgcaa	LCR bridging oligonucleotide to ligate d/s + plasmid backbone of mlc3Δ*act* deletion cassette.
oVPL3216	atcaccaccgaagagatacc	F. *L. reuteri* mlc3Δ*act* deletion cassette screening oligonucleotide.
oVPL3217	agttgggtggataagtatgac	R. *L. reuteri* mlc3Δ*act* deletion cassette screening oligonucleotide.
oVPL3220	ataaaatactattacaaggagattttagccatgcttaatagtaaga gactccactacata	Bridging oligonucleotide to ligate plasmid backbone + *act* gene for *act* gene overexpression cassettes.
oVPL3221	aataaatttgttaggatgataattccttaagaattcggtaccccgg gttcgaaggcgcca	Bridging oligonucleotide to ligate plasmid backbone + *act* gene for *act* gene overexpression cassettes.
oVPL3237	acgtgtctcctatgttaataccg	F. amplifies u/s flanking region of *act* gene in *L. reuteri* DSM17938.
oVPL3238	tataccaaattgtgctggat	R. amplifies u/s flanking region of *act* gene in *L. reuteri* DSM17938.
oVPL3239	aattattcgtataatagttgatcc	F. amplifies d/s flanking region of *act* gene in *L. reuteri* DSM17938.
oVPL3240	ccaactcacttgacccggta	R. amplifies d/s flanking region of *act* gene in *L. reuteri* DSM17938.
oVPL3241	aaacgacggccagtgaattcgagctcggtaacgtgtctcctatg ttaataccggggaaaa	LCR bridging oligonucleotide to ligate plasmid backbone + u/s flanking region of DSM17938Δ*act* deletion cassette.
oVPL3242	actgtaactaatccagcacaatttggtataaattattcgtataatag ttgatcctcttgt	LCR bridging oligonucleotide to ligate u/s + d/s flanking region of DSM17938Δ*act* deletion cassette.
oVPL3243	gttttctttttaccgggtcaagtgagttggatcctctagagtcgacc tgcaggcatgcaa	LCR bridging oligonucleotide to ligate d/s + plasmid backbone of DSM17938Δ*act* deletion cassette.
oVPL3244	gaaattgttcgtcgctatgga	F. *L. reuteri* DSM17938Δ*act* deletion cassette screening oligonucleotide.

oVPL3245	tcccagatttctggccaac	R. *L. reuteri* DSM17938Δ*act* deletion cassette screening oligonucleotide.

oVPL: van Pijkeren Laboratory oligonucleotide identification number. F: Forward, R: Reverse, u/s: upstream, d/s: downstream; LCR: Ligase Cycling Reaction.

Table S5. Plasmids used in this study.

Plasmid	Characteristic	Source
pVPL3002	pORI19 harboring *L. reuteri* derived ddlF258Y	(Zhang et al., 2018)
pVPL31150	pSIP411 harboring *L. reuteri* 6475 *act* gene	This Study
pVPL2042	Em^R, pNZ8048 derivative. Cm marker was replaced by Em marker	(Zhang et al., 2018)
pVPL31130	Em^R, derivative of vector pVPL3002 in which the *L. reuteri* R2lc*::Cm* and R2lcΔ*pks::Cm* insertion cassette was cloned in the MCS site.	This Study
pVPL31079	Em^R, derivative of vector pVPL3002 in which the *L. reuteri* mlc3Δ*act* deletion cassette was cloned in the MCS site.	This Study
pVPL31139	Em^R, derivative of vector pVPL3002 in which the *L. reuteri* DSM17938Δ*act* deletion cassette was cloned in the MCS site.	This Study

pVPL: Van Pijkeren Laboratory plasmid identification number. Em^R: Erythromycin-resistant; Cm^R: Chloramphenicol-resistant. Related to STAR Methods.

Table S6. Acyltransferase gene in *L. reuteri* strains

Host	Host	Strain	Lineage	ACT_genes
Rodent	Mouse (Mus musculus)	480_44	I	No hits found
Rodent	Mouse (Mus musculus)	482_46	I	No hits found
Rodent	Mouse (Mus musculus)	484_39	I	No hits found
Rodent	Mouse	I49	I	No hits found
Rodent	Rat	L106	I	Identities = 102/377 (27%)
Rodent	Rat	L107	I	Identities = 102/377 (27%)
Rodent	Rattus norvegicus	L109	I	Identities = 191/354 (54%)
Rodent	Rattus norvegicus	L110	I	Identities = 191/354 (54%)
Rodent	Rattus norvegicus	L111	I	Identities = 191/354 (54%)
Avian	Cape teal	L5	I	No hits found
Avian	Cape teal	L6	I	No hits found
Rodent	Mouse	lpuph1	I	Identities = 63/246 (26%)
Rodent	Mouse (Mus musculus)	LR0	I	No hits found
Avian	Bird (Gallus gallus)	P43	I	No hits found
Rodent	Rat	TD1	I	Identities = 102/377 (27%)
Human	Human	DSM 20016	II	Identities = 352/355 (99%)
Human	Human (Homo sapiens)	IRT	II	Identities = 352/355 (99%)
Human	Human	JCM1112	II	Identities = 352/355 (99%)
Human	Amaru indians	L26	II	Identities = 193/354 (55%)
Human	Amaru indians	L27	II	Identities = 193/354 (55%)
Human	Human	L28	II	Identities = 352/355 (99%)
Human	Human	L29	II	Identities = 352/355 (99%)
Human	Human	L30	II	Identities = 351/355 (99%)
Human	Human	L31	II	Identities = 351/355 (99%)

Human	Human	L32	II	Identities = 352/355 (99%)
Human	Human	L33	II	Identities = 352/355 (99%)
Human	Human	L37	II	Identities = 352/355 (99%)
Human	Human (Homo sapiens)	MM2-3	II	Identities = 352/355 (99%)
Human	Human (Homo sapiens)	MM4-1a	II	Identities = 352/355 (99%)
Rodent	Rat	100-23	III	No hits found
Rodent	Mouse	103b	III	Identities = 355/355 (100%)
Rodent	Mouse	107k	III	No hits found
Rodent	Mouse	111b	III	Identities = 355/355 (100%)
Rodent	Mouse	609d	III	No hits found
Human	Human (Homo sapiens)	DS12_10	III	No hits found
Rodent	Mouse	L118	III	No hits found
Rodent	Mouse	L119	III	No hits found
Rodent	Mouse	L120	III	Identities = 106/379 (28%)
Human	Amaru indians	L25	III	No hits found
Rodent	Marmota vancouveriensis	L92	III	Identities = 355/355 (100%)
Rodent	Sourdough	LTH2584	III	No hits found
Rodent	Sourdough	LTH5448	III	Identities = 193/354 (55%)
Rodent	Mouse	mlc3	III	Identities = 355/355 (100%)
pig	Pig	ATCC 53608	IV	Identities = 192/354 (54%)
pig	Pig	I5007	IV	Identities = 107/384 (28%)
pig	Pig	KLR1001	IV	Identities = 77/250 (31%)
pig	Pig	KLR2001	IV	Identities = 192/354 (54%)
pig	Pig	KLR3002	IV	No hits found
Primate	Agile gibbon	L123	IV	Identities = 85/321 (26%)
Primate	Lion-tailed Macaque	L125	IV	Identities = 58/152 (38%)
Primate	Orangutan	L126	IV	No hits found
Primate	Japanese macaque	L45	IV	No hits found
Primate	Japanese macaque	L46	IV	No hits found
Primate	Japanese macaque	L47	IV	No hits found
Primate	Agile gibbon	L48	IV	No hits found
Primate	Agile gibbon	L49	IV	No hits found
Primate	Agile gibbon	L50	IV	No hits found
Primate	Gorilla	L55	IV	No hits found
Primate	Sulawesi macaque	L59	IV	No hits found
Primate	Mandrill	L60	IV	No hits found
Primate	Mandrill	L61	IV	No hits found
Primate	Mandrill	L62	IV	No hits found
Primate	Monkey	L68	IV	No hits found
Primate	Monkey	L69	IV	No hits found
Primate	Orangutan	L71	IV	No hits found
Primate	Orangutan	L72	IV	No hits found
Primate	Orangutan	L73	IV	No hits found
pig	Pig	lp167-67	IV	No hits found
pig	Pig	pg-3b	IV	No hits found
pig	Pig	ZLR003	IV	No hits found
pig	Pig	20-2	V	Identities = 97/388 (25%)
pig	Pig	3c6	V	No hits found

Avian	Bird (Gallus gallus)	1366	VI	No hits found
Avian	Gallus gallus	An166	VI	Identities = 97/388 (25%)
Avian	Gallus gallus	An71	VI	Identities = 97/388 (25%)
Human	Human (Homo sapiens)	CF48-3A	VI	Identities = 111/391 (28%)
Avian	Bird (Gallus gallus)	CSF8	VI	No hits found
Human	Homo sapiens	DS17_10	VI	No hits found
Avian	Gallus gallus	JCM1081	VI	No hits found
Avian	African spoonbiil	L1	VI	Identities = 111/391 (28%)
Avian	Golden pheasant	L10	VI	Identities = 82/272 (30%)
Avian	Golden pheasant	L11	VI	Identities = 82/272 (30%)
Avian	Golden pheasant	L12	VI	Identities = 82/272 (30%)
Avian	Poultry	L17	VI	Identities = 97/388 (25%)
Avian	Quail	L19	VI	Identities = 111/391 (28%)
Avian	Argus pheasent	L2	VI	Identities = 197/354 (56%)
Avian	Quail	L20	VI	Identities = 111/391 (28%)
Avian	Quail	L21	VI	Identities = 111/391 (28%)
Avian	Turkey	L22	VI	No hits found
Avian	Turkey	L23	VI	Identities = 352/355 (99%)
Avian	Turkey	L24	VI	Identities = 111/391 (28%)
Avian	Argus pheasent	L3	VI	Identities = 352/355 (99%)
Human	Human	L34	VI	Identities = 111/391 (28%)
Human	Human	L35	VI	Identities = 111/391 (28%)
Human	Human	L36	VI	Identities = 111/391 (28%)
Avian	Argus pheasent	L4	VI	Identities = 352/355 (99%)
Human	Png	L43	VI	Identities = 153/353 (43%)
Avian	Francolin	L7	VI	Identities = 111/391 (28%)
Avian	Francolin	L8	VI	Identities = 111/391 (28%)
Avian	Francolin	L9	VI	Identities = 111/391 (28%)
Human	Human (Homo sapiens)	M27U15	VI	Identities = 111/391 (28%)
Human	Human (Homo sapiens)	MD-IIE-43	VI	No hits found
Human	Human (Homo sapiens)	MM34-4A	VI	Identities = 111/391 (28%)
Human	Human (Homo sapiens)	RC-14	VI	No hits found
Human	Human (Homo sapiens)	SD2112	VI	Identities = 111/391 (28%)
Rodent	Rat	L108	VII	No hits found
Rodent	Springhaas	L112	VII	Identities = 193/354 (55%)
Rodent	Springhaas	L113	VII	Identities = 193/354 (55%)
Rodent	Springhaas	L114	VII	Identities = 193/354 (55%)
Rodent	Porqupine	L121	VII	Identities = 252/355 (71%)
Human	Png	L38	VII	No hits found
Human	Png	L39	VII	No hits found
Human	Png	L40	VII	No hits found
Human	Png	L41	VII	No hits found
Human	Png	L42	VII	No hits found
Human	Png	L44	VII	No hits found
Primate	Black howler monkey	L51	VII	Identities = 193/354 (55%)
Primate	Lion-tailed Macaque	L56	VII	Identities = 109/384 (28%)
Primate	Lion-tailed Macaque	L57	VII	No hits found
Primate	Lion-tailed Macaque	L58	VII	No hits found

Primate	Patas monkey	L65	VII	No hits found
Primate	Monkey	L70	VII	Identities = 254/355 (72%)
Rodent	Capy C	L85	VII	No hits found
Rodent	Capy C	L86	VII	No hits found
Rodent	Coendou prehensilis	L87	VII	No hits found
Rodent	Dasyprocta leporina	L88	VII	No hits found
Rodent	Dasyprocta leporina	L89	VII	No hits found
Primate	Black howler monkey	L124	IX	Identities = 83/329 (25%)
Primate	Black howler monkey	L52	IX	Identities = 83/329 (25%)
Primate	Black howler monkey	L53	IX	Identities = 83/329 (25%)
Primate	Patas monkey	L66	IX	No hits found
Primate	Patas monkey	L67	IX	No hits found
Primate	Mandrill	L63	Close to IX	No hits found
Primate	Mandrill	L64	Close to IX	No hits found
Rodent	Apodemus agrarius	L77	Close to *L. reuteri*	Identities = 106/384 (28%)
Rodent	Apodemus agrarius	L78	Close to *L. reuteri*	Identities = 106/384 (28%)
Rodent	Apodemus agrarius	L79	Close to *L. reuteri*	Identities = 106/384 (28%)
Rodent	Apodemus agrarius	L80	Close to *L. reuteri*	Identities = 106/384 (28%)

Related to Figure 5.

References

Aleti, G., Baker, J.L., Tang, X., Alvarez, R., Dinis, M., Tran, N.C., Melnik, A. V., Zhong, C., Ernst, M., Dorrestein, P.C., et al. (2019). Identification of the Bacterial Biosynthetic Gene Clusters of the Oral Microbiome Illuminates the Unexplored Social Language of Bacteria during Health and Disease. MBio *10*.

Bonder, M.J., Kurilshikov, A., Tigchelaar, E.F., Mujagic, Z., Imhann, F., Vila, A.V., Deelen, P., Vatanen, T., Schirmer, M., Smeekens, S.P., et al. (2016). The effect of host genetics on the gut microbiome. Nat. Genet. *48*, 1407–1412.

Boon, E., Meehan, C.J., Whidden, C., Wong, D.H.-J., Langille, M.G.I., and Beiko, R.G. (2014). Interactions in the microbiome: communities of organisms and communities of genes. FEMS Microbiol. Rev. *38*, 90–118.

Cha, R.S., Zarbl, H., Keohavong, P., and Thilly, W.G. (1992). Mismatch amplification mutation assay (MAMA): Application to the c-H-ras gene. Genome Res. *2*, 14–20.

729 Cimermancic, P., Medema, M.H., Claesen, J., Kurita, K., Wieland Brown, L.C., Mavrommatis,
730 K., Pati, A., Godfrey, P.A., Koehrsen, M., Clardy, J., et al. (2014). Insights into secondary
731 metabolism from a global analysis of prokaryotic biosynthetic gene clusters. Cell *158*, 412–421.
732 David, L.A., Maurice, C.F., Carmody, R.N., Gootenberg, D.B., Button, J.E., Wolfe, B.E., Ling,
733 A. V, Devlin, A.S., Varma, Y., Fischbach, M.A., et al. (2014). Diet rapidly and reproducibly
734 alters the human gut microbiome. Nature *505*, 559–563.
735 Donia, M.S., Cimermancic, P., Schulze, C.J., Wieland Brown, L.C., Martin, J., Mitreva, M.,
736 Clardy, J., Linington, R.G., and Fischbach, M.A. (2014). A Systematic Analysis of Biosynthetic
737 Gene Clusters in the Human Microbiome Reveals a Common Family of Antibiotics. Cell *158*,
738 1402–1414.
739 Duar, R.M., Frese, S.A., Lin, X.B., Fernando, S.C., Burkey, T.E., Tasseva, G., Peterson, D.A.,
740 Blom, J., Wenzel, C.Q., Szymanski, C.M., et al. (2017). Experimental Evaluation of Host
741 Adaptation of Lactobacillus reuteri to Different Vertebrate Species. Appl. Environ. Microbiol.
742 *83*, e00132-17.
743 Edgar, R.C. (2004). MUSCLE: Multiple sequence alignment with high accuracy and high
744 throughput. Nucleic Acids Res. *32*, 1792–1797.
745 Edwards, K.F., Kremer, C.T., Miller, E.T., Osmond, M.M., Litchman, E., and Klausmeier, C.A.
746 (2018). Evolutionarily stable communities: a framework for understanding the role of trait
747 evolution in the maintenance of diversity. Ecol. Lett. *21*, 1853–1868.
748 Frese, S.A., Benson, A.K., Tannock, G.W., Loach, D.M., Kim, J., Zhang, M., Oh, P.L., Heng,
749 N.C.K., Patil, P.B., Juge, N., et al. (2011). The evolution of host specialization in the vertebrate
750 gut symbiont Lactobacillus reuteri. PLoS Genet. *7*.
751 Frese, S.A., MacKenzie, D.A., Peterson, D.A., Schmaltz, R., Fangman, T., Zhou, Y., Zhang, C.,

752 Benson, A.K., Cody, L.A., Mulholland, F., et al. (2013). Molecular Characterization of Host-
753 Specific Biofilm Formation in a Vertebrate Gut Symbiont. PLoS Genet. *9*.
754 Le Gac, M., Plucain, J., Hindré, T., Lenski, R.E., and Schneider, D. (2012). Ecological and
755 evolutionary dynamics of coexisting lineages during a long-term experiment with Escherichia
756 coli. Proc. Natl. Acad. Sci. U. S. A. *109*, 9487–9492.
757 Gruber, G., and Steglich, W. (2007). Calostomal, a polyene pigment from the gasteromycete
758 Colostoma cinnabarinum (Boletales). Zeitschrift Fur Naturforsch. - Sect. B J. Chem. Sci. *62*,
759 129–131.
760 Ha, R., Frirdich, E., Sychantha, D., Biboy, J., Taveirne, M.E., Johnson, J.G., DiRita, V.J.,
761 Vollmer, W., Clarke, A.J., and Gaynor, E.C. (2016). Accumulation of Peptidoglycan *O* -
762 Acetylation Leads to Altered Cell Wall Biochemistry and Negatively Impacts Pathogenesis
763 Factors of *Campylobacter jejuni*. J. Biol. Chem. *291*, 22686–22702.
764 Herbrík, A., Corretto, E., Chroňáková, A., Langhansová, H., Petrásková, P., Hrdý, J., Čihák, M.,
765 Krištůfek, V., Bobek, J., Petříček, M., et al. (2020). A Human Lung-Associated Streptomyces sp.
766 TR1341 Produces Various Secondary Metabolites Responsible for Virulence, Cytotoxicity and
767 Modulation of Immune Response. Front. Microbiol. *10*, 3028.
768 Hibbing, M.E., Fuqua, C., Parsek, M.R., and Peterson, S.B. (2010). Bacterial competition:
769 surviving and thriving in the microbial jungle. Nat. Rev. Microbiol. *8*, 15–25.
770 Hiergeist, A., Gläsner, J., Reischl, U., and Gessner, A. (2015). Analyses of Intestinal Microbiota:
771 Culture versus Sequencing. ILAR J. *56*, 228–240.
772 Hooper, L. V, Littman, D.R., Macpherson, A.J., and Program, M.P. (2015). Interactions between
773 the microbiota and the immune system. Science (80-.). *336*, 1268–1273.
774 Hou, Y., Braun, D.R., Michel, C.R., Klassen, J.L., Adnani, N., Wyche, T.P., and Bugni, T.S.

775 (2012). Microbial Strain Prioritization Using Metabolomics Tools for the Discovery of Natural
776 Products. Anal. Chem. *84*, 4277–4283.
777 Jacobson, A., Lam, L., Rajendram, M., Tamburini, F., Honeycutt, J., Pham, T., Van Treuren, W.,
778 Pruss, K., Stabler, S.R., Lugo, K., et al. (2018). A Gut Commensal-Produced Metabolite
779 Mediates Colonization Resistance to Salmonella Infection. Cell Host Microbe *24*, 296–307.e7.
780 Kok, S. De, Stanton, L.H., Slaby, T., Durot, M., Holmes, V.F., Patel, K.G., Platt, D., Shapland,
781 E.B., Serber, Z., Dean, J., et al. (2014). Rapid and reliable DNA assembly via ligase cycling
782 reaction. ACS Synth. Biol. *3*, 97–106.
783 Kumar, S., Stecher, G., Li, M., Knyaz, C., and Tamura, K. (2018). MEGA X: Molecular
784 Evolutionary Genetics Analysis across Computing Platforms. Mol. Biol. Evol. *35*, 1547–1549.
785 Lee, A.J., Cadelis, M.M., Kim, S.H., Swift, S., Copp, B.R., and Villas-Boas, S.G. (2020).
786 Epipyrone A, a Broad-Spectrum Antifungal Compound Produced by Epicoccum nigrum ICMP
787 19927. Molecules *25*, 5997.
788 Leenhouts, K., Buist, G., Bolhuis, A., Berge, A. ten, Kiel, J., Mierau, I., Dabrowska, M.,
789 Venema, G., and Kok, J. (1996). A general system for generating unlabelled gene replacements
790 in bacterial chromosomes. Mol. Gen. Genet. MGG *253*, 217–224.
791 Li, J., Sang, M., Jiang, Y., Wei, J., Shen, Y., Huang, Q., Li, Y., and Ni, J. (2021). Polyene-
792 Producing Streptomyces spp. From the Fungus-Growing Termite Macrotermes barneyi Exhibit
793 High Inhibitory Activity Against the Antagonistic Fungus Xylaria. Front. Microbiol. *12*, 649962.
794 Lin, X.B., Lohans, C.T., Duar, R., Zheng, J., Vederas, J.C., Walter, J., and Gänzle, M. (2015).
795 Genetic determinants of reutericyclin biosynthesis in Lactobacillus reuteri. Appl. Environ.
796 Microbiol. *81*, 2032–2041.
797 Lin, X.B., Wang, T., Stothard, P., Corander, J., Wang, J., Baines, J.F., Knowles, S.C.L.,

798 Baltrūnaitė, L., Tasseva, G., Schmaltz, R., et al. (2018). The evolution of ecological facilitation
799 within mixed-species biofilms in the mouse gastrointestinal tract. ISME J. 1.
800 Martínez, I., Maldonado-Gomez, M.X., Gomes-Neto, J.C., Kittana, H., Ding, H., Schmaltz, R.,
801 Joglekar, P., Cardona, R.J., Marsteller, N.L., Kembel, S.W., et al. (2018). Experimental
802 evaluation of the importance of colonization history in early-life gut microbiota assembly. Elife
803 *7*.
804 Medema, M.H., Blin, K., Cimermancic, P., de Jager, V., Zakrzewski, P., Fischbach, M.A.,
805 Weber, T., Takano, E., and Breitling, R. (2011). antiSMASH: rapid identification, annotation and
806 analysis of secondary metabolite biosynthesis gene clusters in bacterial and fungal genome
807 sequences. Nucleic Acids Res. *39*, W339-46.
808 Medema, M.H., Cimermancic, P., Sali, A., Takano, E., and Fischbach, M.A. (2014). A
809 Systematic Computational Analysis of Biosynthetic Gene Cluster Evolution: Lessons for
810 Engineering Biosynthesis. PLoS Comput. Biol. *10*.
811 Moynihan, P.J., and Clarke, A.J. (2010). O-acetylation of peptidoglycan in gram-negative
812 bacteria: identification and characterization of peptidoglycan O-acetyltransferase in Neisseria
813 gonorrhoeae. J. Biol. Chem. *285*, 13264–13273.
814 Murray, I.A., and Shaw, W. V. (1997). O-Acetyltransferases for chloramphenicol and other
815 natural products. Antimicrob. Agents Chemother. *41*, 1–6.
816 Oh, J.H., and Van Pijkeren, J.P. (2014). CRISPR-Cas9-assisted recombineering in Lactobacillus
817 reuteri. Nucleic Acids Res. *42*.
818 Oh, J.-H., Lin, X.B., Zhang, S., Tollenaar, S.L., Özçam, M., Dunphy, C., Walter, J.E., and
819 Pijkeren, J.-P. van (2019). Prophages in Lactobacillus reuteri are associated with fitness trade-
820 offs but can increase competitiveness in the gut ecosystem. Appl. Environ. Microbiol.

821 Oh, P.L., Benson, A.K., Peterson, D.A., Patil, P.B., Moriyama, E.N., Roos, S., and Walter, J.
822 (2009). Diversification of the gut symbiont Lactobacillus reuteri as a result of host-driven
823 evolution. ISME J. *4*, 377–387.
824 Özçam, M., and van Pijkeren, J.-P. (2019). Draft Genome Sequence of Aryl Hydrocarbon
825 Receptor Activator Strains Lactobacillus reuteri R2lc and 2010 . Microbiol. Resour. Announc. *8*.
826 Özçam, M., Tocmo, R., Oh, J.H., Afrazi, A., Mezrich, J.D., Roos, S., Claesen, J., and van
827 Pijkeren, J.P. (2019). Gut symbionts Lactobacillus reuteri R2lc and 2010 encode a polyketide
828 synthase cluster that activates the mammalian aryl hydrocarbon receptor. Appl. Environ.
829 Microbiol. *85*.
830 Van Pijkeren, J.P., and Britton, R.A. (2012). High efficiency recombineering in lactic acid
831 bacteria. Nucleic Acids Res. *40*, 1–13.
832 Van Pijkeren, J.-P., Neoh, K.M., Sirias, D., Findley, A.S., and Britton, R.A. (2012). Exploring
833 optimization parameters to increase ssDNA recombineering in Lactococcus lactis and
834 Lactobacillus reuteri. Bioengineered *3*, 209–217.
835 Ragland, S.A., and Criss, A.K. (2017). From bacterial killing to immune modulation: Recent
836 insights into the functions of lysozyme. PLoS Pathog. *13*, e1006512.
837 Sambrook, J., and Russell, D.W. (2006). Transformation of *E. coli* by Electroporation. Cold
838 Spring Harb. Protoc. *2006*, pdb.prot3933.
839 Sassone-Corsi, M., Nuccio, S.-P., Liu, H., Hernandez, D., Vu, C.T., Takahashi, A.A., Edwards,
840 R.A., and Raffatellu, M. (2016). Microcins mediate competition among Enterobacteriaceae in the
841 inflamed gut. Nature *540*, 280–283.
842 Savage, D.C., Dubos, R., and Schaedler, R.W. (1968). The gastrointestinal epithelium and its
843 autochthonous bacterial flora. J. Exp. Med. *127*, 67–76.

844 Sender, R., Fuchs, S., and Milo, R. (2016). Revised Estimates for the Number of Human and
845 Bacteria Cells in the Body. PLoS Biol. *14*, e1002533.
846 Snijders, A.M., Langley, S.A., Kim, Y.-M., Brislawn, C.J., Noecker, C., Zink, E.M., Fansler,
847 S.J., Casey, C.P., Miller, D.R., Huang, Y., et al. (2016). Influence of early life exposure, host
848 genetics and diet on the mouse gut microbiome and metabolome. Nat. Microbiol. *2*, 16221.
849 Turnbaugh, P.J., Ridaura, V.K., Faith, J.J., Rey, F.E., Knight, R., and Gordon, J.I. (2009). The
850 effect of diet on the human gut microbiome: a metagenomic analysis in humanized gnotobiotic
851 mice. Sci. Transl. Med. *1*, 6ra14.
852 Vaishnava, S., Yamamoto, M., Severson, K.M., Ruhn, K.A., Yu, X., Koren, O., Ley, R.,
853 Wakeland, E.K., and Hooper, L. V. (2011). The antibacterial lectin RegIIIγ promotes the spatial
854 segregation of microbiota and host in the intestine. Science (80-.). *334*, 255–258.
855 Veldhoen, M., Hirota, K., Westendorf, A.M., Buer, J., Dumoutier, L., Renauld, J.-C., and
856 Stockinger, B. (2008). The aryl hydrocarbon receptor links TH17-cell-mediated autoimmunity to
857 environmental toxins. Nature *453*, 106–109.
858 Vollmer, W. (2008). Structural variation in the glycan strands of bacterial peptidoglycan. FEMS
859 Microbiol. Rev. *32*, 287–306.
860 Walter, J., Britton, R.A., and Roos, S. (2011). Host-microbial symbiosis in the vertebrate
861 gastrointestinal tract and the Lactobacillus reuteri paradigm. Proc. Natl. Acad. Sci. *108*, 4645–
862 4652.
863 Youngblut, N.D., De La Cuesta-Zuluaga, J., Reischer, G.H., Dauser, S., Schuster, N., Walzer, C.,
864 Stalder, G., Farnleitner, A.H., and Ley, R.E. (2020). Large-Scale Metagenome Assembly
865 Reveals Novel Animal-Associated Microbial Genomes, Biosynthetic Gene Clusters, and Other
866 Genetic Diversity.

867 Zarrinpar, A., Chaix, A., Yooseph, S., and Panda, S. (2014). Diet and feeding pattern affect the
868 diurnal dynamics of the gut microbiome. Cell Metab. *20*, 1006–1017.
869 Zhang, S., Oh, J.-H., Alexander, L.M., Özçam, M., and Van Pijkeren, J.-P. (2018). D-Ala-D-Ala
870 ligase as a broad host-range counterselection marker in vancomycin-resistant lactic acid bacteria.
871 J. Bacteriol. JB.00607-17.
872 Zhao, W.T., Shi, X., Xian, P.J., Feng, Z., Yang, J., and Yang, X.L. (2021). A new fusicoccane
873 diterpene and a new polyene from the plant endophytic fungus Talaromyces pinophilus and their
874 antimicrobial activities. Nat. Prod. Res. *35*, 124–130.
875 Zheng, J., Wittouck, S., Salvetti, E., Franz, C.M.A.P., Harris, H.M.B., Mattarelli, P., O'toole,
876 P.W., Pot, B., Vandamme, P., Walter, J., et al. (2020). A taxonomic note on the genus
877 Lactobacillus: Description of 23 novel genera, emended description of the genus Lactobacillus
878 beijerinck 1901, and union of Lactobacillaceae and Leuconostocaceae. Int. J. Syst. Evol.
879 Microbiol. *70*, 2782–2858.
880 Zheng, Y., Valdez, P.A., Danilenko, D.M., Hu, Y., Sa, S.M., Gong, Q., Abbas, A.R., Modrusan,
881 Z., Ghilardi, N., de Sauvage, F.J., et al. (2008). Interleukin-22 mediates early host defense
882 against attaching and effacing bacterial pathogens. Nat. Med. *14*, 282–289.
883